D1 - Numerical and experimental evidence and review of methods prescribed by codes for the seismic input definition on NSCs

ABSTRACT

This document is the first Deliverable (D1) of the "NEWTON – NEWTOols to compute the seismic demand on Non-structural components" project. It provides the project state of the art and it includes: i) a literature review of numerical studies and experimental shake-table tests, to identify the parameters mostly affecting the estimation of the seismic demands on nonstructural components and their effects on amplitude and shape of floor response spectra; ii) a review of methods prescribed by codes, highlighting those which explicitly consider the influential parameters identified in the previous step. The main outcome of D1 is the definition of a database of experimental shake-table tests performed in the last decade, summarizing prototype and test set-up main features, data collected during the tests, investigated parameters, and main trends observed. The sources are clarified, specifying if the test results are available or not for further evaluation.

Document versions:

Authors	Actions	Date
Degli Abbati S, Ricci P, Di Domenico M, Parisse F	First drafting, review and editing	**22/04/2024**

Cite this Deliverable:

Degli Abbati S, Ricci P, Di Domenico M, Parisse F. (2024). Numerical and experimental evidence and review of methods prescribed by codes for the seismic input definition on NSCs. Deliverable 1 of the "NEWTON – NEWTOols to compute the seismic demand on Non-structural components" project. University of Napoli Federico II and University of Genova. Draft of 22/04/2024. URL: https://www.newton-prin.it/en/deliverables.html

TABLE OF CONTENTS

1 Introduction

Nonstructural components (NSCs) are not crucial for structural integrity, nor they are a part of the structural load-resisting system, and therefore their seismic response can be considered separately. Typical examples are partition walls (specifically in the out-of-plane direction) or parapets, which are relevant for the building functionality, but also pinnacles or artistic assets, which can have a remarkable value in monumental buildings due to their economic and cultural importance. Damage to NSCs is a recurring topic (Filiatrault and Sullivan 2014; Perrone et al. 2019), even when considering seismic intensities lower than those producing structural damage, and its repercussions are critical from cultural and monetary loss and life-safety risk perspectives (Figure 1). According to FEMA 356 2000, NSCs are generally classified depending on their seismic response into deformation-sensitive (*e.g.,* infill walls in their in-plane direction) and acceleration-sensitive NSCs (*e.g.,* parapets, chimneys, and infill walls under out-of-plane actions). This Deliverable focuses on the acceleration-sensitive NSCs that can be typically found in Reinforced Concrete (RC) and masonry buildings.

Figure 1. Post-earthquake damage to NSCs in reinforced concrete and masonry buildings.

The seismic input acting at the base of an NSC housed in a building is defined as Floor Response Spectra (FRS) at the position and height where the component is attached to the building. FRS are generated from the absolute acceleration of a floor in a building that is excited by the input ground motion, as sketched in Figure 2. The supporting structure filters out the vibrational components with frequencies different from the building's frequencies, whereas the vibrational components with frequencies close to the natural frequencies are amplified (Sullivan et al. 2013b). This phenomenon is rather complex, being influenced by the characteristics of ground motion excitation, supporting structure, and NSCs. Thus, FRS have attracted the attention of researchers worldwide in the last few decades, and significant efforts have been made to understand better the parameters influencing them.

In this context, this Deliverable aims at providing the state of the art of project "NEWTON – NEWTOols to compute the seismic demand on Non-structural components", recently funded by Italian Ministry of University and Research in the framework of the 2022 PRIN (*Progetti di Rilevante Interesse Nazionale*). To this aim, the Deliverable is organized into two main Sections: Section 2 presents a state-of-the-art review of numerical and experimental studies performed in the recent past to investigate the amplification phenomenon; Section 3 reviews and compares the main code

prescriptions for the FRS definition, highlighting those which explicitly consider the influential parameters identified in Section 2.

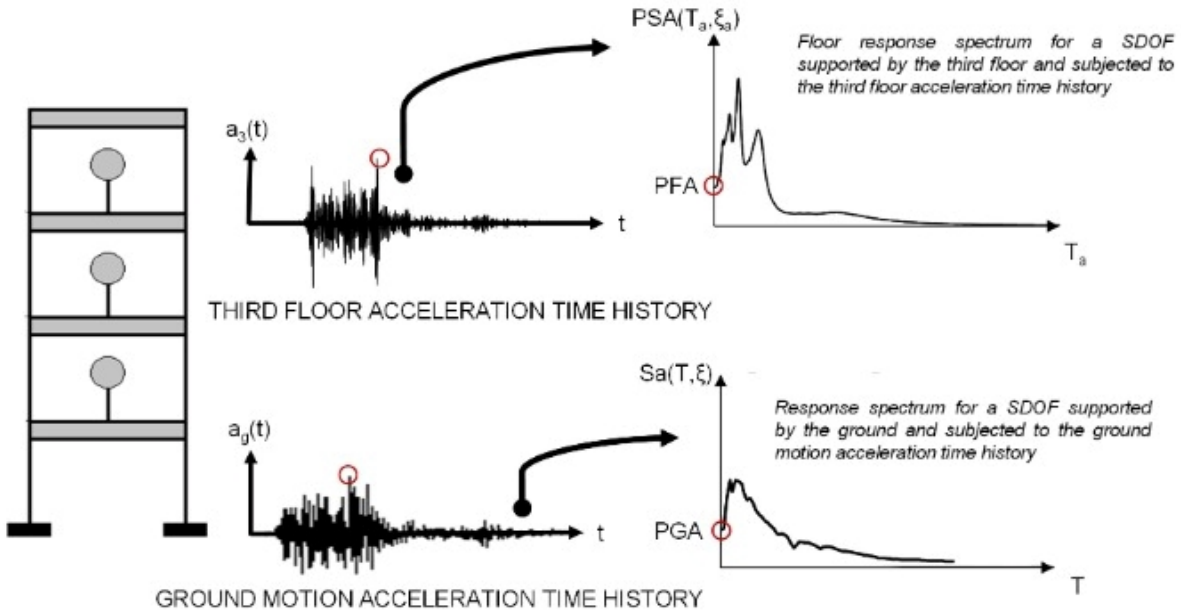

Figure 2. Definition of FRS (figure adapted from Di Domenico et al. 2021).

2 Literature review of past numerical and experimental studies

This Section provides a critical review of numerical studies and recently performed experimental shake-table tests to investigate the amplification phenomenon. First, the different methods for generating FRS will be summarized in Section 2.1. Then, a review of the parameters influencing FRS will be presented in Section 2.2, trying to assess their main effects on FRS. These parameters include the characteristics of the ground motion, supporting building, and NSCs. Finally, a review of shake-table tests performed in the last decade to assess seismic demands on NSCs will be presented in Section 2.3. As the main output of Section 2.3, an open-access database of past experimental campaigns is defined and attached to this Deliverable.

2.1 Development of floor response spectra

According to Wang et al. 2021, four methods can be used to define FRS, *i.e.,* FRS based on Single-Degree-Of-Freedom (SDOF) models, FRS based on Multiple-Degree-Of-Freedom (MDOF) models, amplification factor methods, and directly defined FRS (see Figure 3, as adapted from Wang et al. 2021). A brief description of each method is reported below, while for more details the interested reader can refer to Wang et al. 2021.

The initial methods (dating back to the 1970s) fall in the first category (FRS based on SDOF models). In these methods, the supporting structure and the NSCs are considered SDOF systems, and the basic parameters considered are the fundamental period, the damping ratio, and the yield strength ratio. SDOF models cannot be accurate in describing the actual response of multi-storey buildings. Thus, more recently, different methods were developed for generating FRS based on MDOF structural models (second category). In these methods, FRS are first generated for each mode and

then combined using a modal superposition technique to obtain the final FRS and consider the effect of different vibration modes. To ease the FRS application, some methods were developed based on the ground acceleration response spectrum (GRS) or the peak ground acceleration (PGA). These methods fall in the third (amplification factor methods) and fourth (directly defined FRS) categories. In some cases, FRS based on MDOF structural models are derived as empirical formulations based on data from nonlinear dynamic analyses of MDOFs, without a theoretical-based explicit distinction between different modal contributions. In the amplification factor methods, the FRS is generated from the GRS by applying an amplification factor which is defined as the ratio of the FRS to the GRS. In the directly defined FRS methods, the FRS is directly calculated using a component acceleration factor defined as FRS/PGA for a given level of PGA.

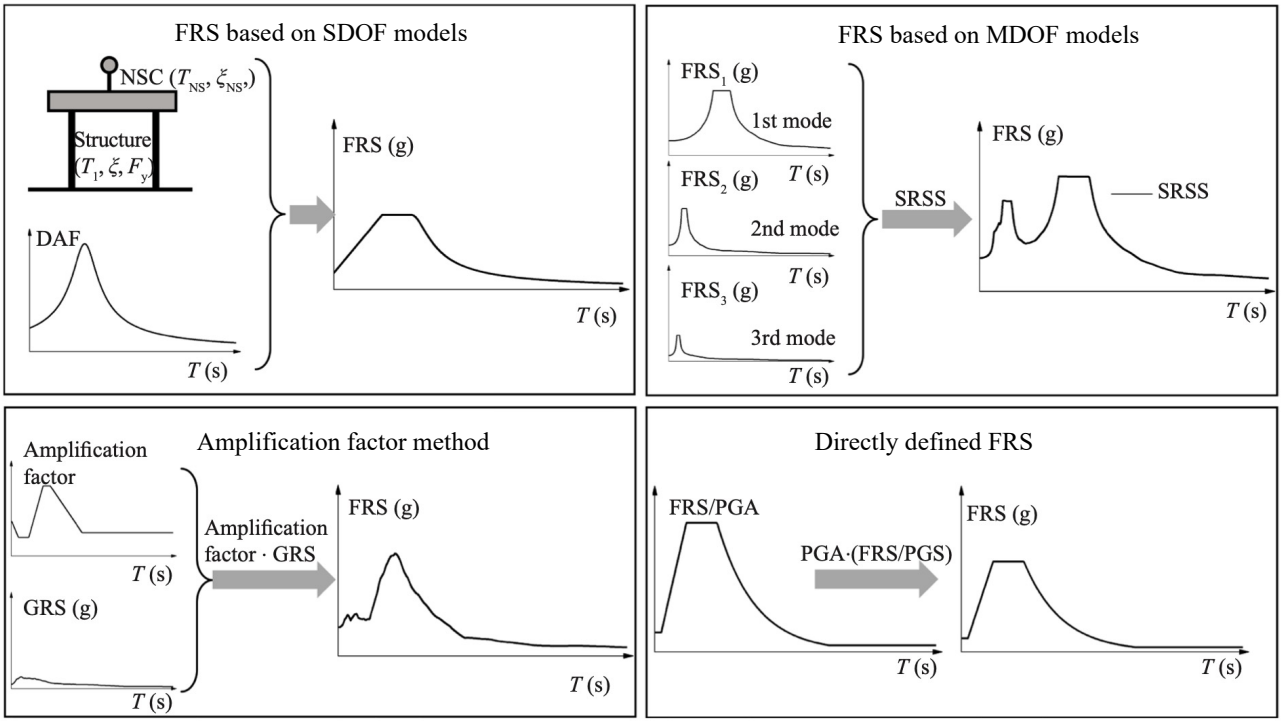

Figure 3. Definition of the four methods available to define FRS according to Wang et al. 2021 (figure adapted from that paper).

2.2 Parameters influencing the floor response spectra

The seismic input acting on an NSC located at a certain level of a building is greatly influenced by the properties of both the supporting structure and the NSC itself, which act as two filters connected in series. The supporting structure first filters the ground excitation. Due to this filtering effect, the characteristics of floor acceleration motions (*i.e.,* the induced motions at the base of the element) are markedly different from those of typical ground accelerations. As a second filter, a NSC can further alter the characteristics of the induced floor acceleration motions. The main parameters influencing the FRS are listed in Table 1. They include the characteristics of the supporting structures, the NSCs, and the interaction effect between the NSCs and the supporting structural components. A detailed

discussion of these influential factors is provided in the review paper by Wang et al. 2021 and summarized below. Since this state-of-the-art review comprises research studies up to 2019, the description is integrated with the main outcomes of the research works developed in the past three years.

Table 1. Parameters that mostly influence FRS.

Factors	**Influencing parameter**
Supporting structure	• Dynamic response • Nonlinear behaviour • In-plane diaphragm flexibility and torsional response
NSC	• Damping ratio • Nonlinear behaviour
Interaction	• Between the structural components and infill walls • Between NSC and the supporting structure
Ground motion excitation	• Vertical component • Near-fault pulse-like ground motion

2.2.1 Effects of the characteristics of the supporting structure

The characteristics of the supporting structure have a significant influence on the FRS.

The **dynamic response** of the building filters the ground excitation at its predominant frequencies of vibration. As a result, FRS are characterized by distinct peaks analogous to contributing modes and with progressively increasing values for increasing floors (*e.g.,* Landge and Ingle 2021). While it is worth noting that responses under various natural vibration modes are superimposed in different proportions to describe the structure's dynamic behaviour, in regular buildings with sufficiently stiff diaphragms and without significant torsional modes, response under the first mode prevails, and the effects of higher vibration modes may be irrelevant (Menon and Magenes 2011a-b).

When the **building** experiences its **nonlinear response**, the peak values of the FRS are generally reduced, except for some cases such as low-damping non-tuned NSCs in buildings with localized plasticity (Lin and Mahin 1985; Toro et al. 1989; Chaudhuri and Villaverde 2008; Sankaranarayanan and Medina 2008; Anajafi 2018). The effects of the nonlinear behaviour of the supporting structure have been investigated in several studies. Sewell et al. 1986 conducted one of the earliest comprehensive studies to identify the factors affecting FRS in nonlinear MDOF structures. They found that SDOF light equipment attached to nonlinear SDOF structures tends to experience lower forces due to the nonlinearity within the structure. However, they also observed discrepancies in the nonlinear behaviour of actual MDOF structures when represented by SDOF systems at higher frequencies. Finally, they demonstrated that the amplification of FRS peaks is influenced by the localized nonlinear behaviour occurring in the supporting structure. Rodriguez et al. 2002 carried out an analytical study on earthquake-induced floor horizontal accelerations in regular buildings with rigid diaphragms. Their findings indicated that the highest magnification of floor acceleration consistently

takes place on the uppermost floor. Moreover, they concluded that a significant reduction in floor accelerations at this level can be expected immediately after the elastic limit. The inelastic response of the supporting structure reduces the floor response around the natural periods of vibrations and the maximum reduction occurs around the first-mode period. Similarly, Kingston 2004 carried out nonlinear time-history analyses on multi-storied regular frames and observed that frame inelastic response primarily affects the first mode. Floros 2006 carried out nonlinear time-history analyses on reinforced concrete frames to study the effect of the nonlinear response of the supporting structure. The analyses showed the importance of tuning the NSC response to the primary structure's second mode. They consistently observed a whip-lash effect at the topmost floor of tall frames, while a constant distribution of Peak Floor Accelerations (PFA) akin to a first-mode shape is observed over the rest of the frame's height. In the parametric studies by Chaudhuri and Villaverde 2008, the authors observed that the peak acceleration response of a linear NSC may increase when the supporting structure goes from linear to localized nonlinear behaviour rather than from linear to widespread nonlinear behaviour. Moreover, it can be expected that NSCs attached to lower floors of a nonlinear supporting structure and tuned to one of its higher modes experience an increased seismic demand. Using simple 1DOF models, Politopoulos and Feau 2007 observed that all three investigated nonlinear behaviours (elastoplastic, origin-oriented, and nonlinear elastic) significantly reduce the FRS peak values, which occur close to the building frequency. They observed that this is not true for the entire range of frequencies depending on the assumed nonlinear behaviour.
Sankaranarayanan 2007 and Sankaranarayanan and Medina 2007 showed that a reduction of FRS values occurred with structural nonlinearity when the period of NSC is close to the building's modal period. A greater reduction was observed near the fundamental period region than in the higher modal period. In addition, an increase in the FRS values was observed between two modal periods of the building. Chaudhuri and Hutchinson 2011 found that the contribution of higher modes increases with building inelasticity which could result in a decrease in the ratio between PFA and PGA values. Anajafi et al. 2022 examined the recorded floor acceleration responses of a wide variety of instrumented budlings to validate the effects of different parameters on FRS as obtained by past numerical studies. They found that building inelastic behaviour usually mitigates the harmonics dominating the floor acceleration responses (especially those with periods close to the first-mode period of the building) reducing the spikes of FRS.

In conclusion, a structure can be considered as a band-pass filter in terms of the ground motion frequency content transmitted to the supported NSCs. The highest amplification of PFA is registered at the top floor level. If a structure experiences its nonlinear response during an earthquake, namely with occurrence of damage, a reduction of the FRS is typically expected. This reduction is likely to occur in correspondence of the fundamental period of the supporting structure.

Further parameters of the supporting structure affecting FRS are the so-called three-dimensional effects (Anajafi and Medina 2019), *i.e.,* the in-plane **diaphragm flexibility** and the **torsional response**.
Diaphragm flexibility is a function of the geometry and structural details of the floor diaphragm as well as the stiffness of the lateral force-resisting system (LFRS). Consequentially, it is a relative term based

on the ratio of the diaphragm in-plane stiffness to the LFRS stiffness. Thus, a given diaphragm could be classified as rigid in one building and flexible in another building. The consequences of diaphragm flexibility are generally more dominant in stiff buildings.

As summarized by Anajafi and Medina 2019 and based on previous studies (*e.g.,* Reinhorn et al. 1988, Kunnath et al. 1991, Iverson and Hawkins 1994, Tena-Colunga and Abrams 1996, Fleischman et al. 1998, Cohen et al. 2001, Fleischman and Farrow 2001, Fleischman et al. 2002, Sadashiva et al. 2012, Tena-Colunga et al. 2015), the effects of diaphragm flexibility can be classified in three categories:

- *Global effects on the building*: diaphragm flexibility alters the building's dynamic behavior and introduces additional degrees of freedom. This can potentially add some higher modes. Furthermore, it increases the modal periods of a building. Depending on the period of the building with a rigid diaphragm assumption and the ground motion frequency content, diaphragm flexibility may have detrimental or beneficial global effects (Tena-Colunga et al. 2015). If the period of the building with a rigid diaphragm assumption lies on the ascending portion of the ground spectrum, the period elongation caused by diaphragm flexibility may result in increased spectral acceleration responses. If the period elongation shifts the building into the descending portion of the ground spectrum, the opposite effect will be observed.
- *Local effects on the diaphragm itself*: diaphragm flexibility can magnify accelerations (as well as displacements, bending moments, and shear forces) at different locations of a floor.
- *Local effects on other components*: diaphragm flexibility can impose large deformations on elements perpendicular to the direction of seismic loading.

Seismic-induced torsional responses in buildings instead occur because of a variety of factors, that can be grouped into three main categories (*e.g.,* Anagnostopoulos et al. 2015):

- The asymmetric arrangement of the stiffness and strength of the LFRS and/or the asymmetric distribution of floors' masses.
- The torsional components of earthquake ground motions.
- The eccentricities between the centers of rigidity and mass that exist because of uncertainties in quantifying the mass and stiffness distribution of a building.

The effects of diaphragm flexibility and torsional responses on FRS have been investigated in different literature studies. Çelebi et al. 1989 analyzed a single-story instrumented building with a flexible diaphragm subjected to a ground motion from the 1984 Morgan Hill earthquake. They showed that the amplification of the roof PFA at the center of the diaphragm with respect to edges was about 3.0. Tena-Colunga and Abrams 1996 evaluated the responses of two instrumented buildings (two-story unreinforced masonry and timber buildings) with flexible diaphragms during the 1989 Loma Prieta earthquake and the simulated responses of the counterpart numerical buildings with rigid diaphragms. They showed that diaphragm flexibility, in addition to increasing displacement responses, could increase PFA responses by a factor up to 2.0 for the studied cases. They also showed that torsional responses could reduce considerably as the diaphragm flexibility increases. In a study conducted by Qu et al. 2014 on a group of instrumented buildings ranging from low to high rise, it was shown that torsion and diaphragm flexibility can amplify PFA responses by factors up to 2.2 and 1.6, respectively.

Bernal et al. 2014 investigated the effect of diaphragm flexibility on floor spectra of a five-story instrumented building subjected to a record from the 2008 Chino Hills earthquake. They showed that the rigid floor assumption was valid for NSC periods below 0.5 s, whereas for longer periods, floor diaphragms did not behave as rigid in their plane. Kollerathu and Menon 2017 performed time history analyses of elastic and inelastic masonry structures, finding that PFA responses increased with increasing the diaphragm flexibility. Anajafi and Medina 2019 computed the FRS of 118 instrumented building in California, selected to encompass a wide range of characteristics (*e.g.,* LFRS, modal periods, level of inelastic behaviour) and recorded ground motion characteristics. They found that the in-plane diaphragm flexibility can produce larger floor acceleration around the middle of a floor plan and that even regular buildings exhibited torsional behaviour and diaphragm flexibility that may increase force demands on NSCs by factors up to 2.0.

Derakhshan et al. 2022 analysed empirical data from nine buildings instrumented by the Centre for Engineering Strong Motion Data (CESMD 2019) to qualitative evaluate the effects of diaphragm flexibility and then performed a series of pushover and incremental dynamic analyses of equivalent frame models of four building typologies. They found that accelerations in buildings with flexible diaphragms are amplified by up to 3 when compared to the case of buildings with rigid diaphragms.

Jain and Surana 2022 investigated a series of reinforced concrete frame buildings with torsional irregularities, subjected to bi-directional earthquake excitations. They analyzed the floor torsional amplification factors (TAFs), defined as the ratio between the floor spectral ordinate at the flexible/stiff edge and that at the center of rigidity. Their findings revealed that TAFs are dependent on building torsional characteristics and tuning ratio, with the most critical values occurring for the flexible NSCs. Peak torsional amplification typically arises when the NSC is tuned to either the translational or torsional modes of building vibration. Additionally, they observed that torsional amplification generally occurs at the flexible edge for both rigid and flexible NSCs, although the potential for amplification at the stiff edge cannot be dismissed. Conversely, TAFs approach values around 1 for very flexible NSCs regardless of building or NSC characteristics. Furthermore, they observed that the damping ratio of NSCs has a limited effect on peak TAFs. Landge and Ingle 2021 carried out an analytical study on low-rise building models subjected to different ground motions to quantify the acceleration floor amplification. The elastic and inelastic acceleration response of regular buildings were obtained as well as the one of buildings characterized by mass and stiffness irregularity. The results showed that mass irregularity at lower storey and the presence of geometric irregularity in buildings amplified the floor acceleration response. In a more recent research work (Landge and Ingle 2022), the authors performed nonlinear dynamic analyses on reinforced concrete frame buildings. Their analyses revealed that even a minor mass eccentricity in structures with regular geometry and uniform stiffness leads to a notable increase in FRS. Additionally, in buildings characterized by substantial variations in mass, stiffness, and strength — such as industrial structures — the FRS are further intensified. Ruggieri and Vukobratovic 2023 developed an extensive parametric study on reinforced concrete single-storey buildings by varying geometrical parameters for inducing different levels of diaphragm flexibility, quantified through the commonly used in-plane displacement ratio. In all the cases considered, diaphragm flexibility significantly influences PFAs and FRS, which can both increase and decrease compared to buildings with rigid diaphragms. In detail, the more flexible parts of buildings

exhibited higher PFAs, while the more rigid parts of buildings had smaller PFAs. In the case of FRS, a shifting of peaks was observed as well.

When summarizing the effects of diaphragm flexibility on the PFA, an amplification trend is found for buildings with flexible floors, especially at the floor center. Since in-plane diaphragm flexibility increase the building modal periods, it could have detrimental or beneficial global effects depending on the corresponding fundamental period and ground motion frequency contents. Torsional effects are correlated with diaphragm flexibility although they are also dependent on the stiffness of vertical structural elements and distribution of masses. However, these effects result in amplification of PFA and floor acceleration responses.

2.2.2 Effects of the characteristics of the NSC

The influence of the **nonlinear behaviour** of the NSC on FRS consists of a reduction in the demand, generally speaking, as well known from the fundamentals of earthquake engineering for nonlinear SDOF systems. It is possible to look at this phenomenon, when dealing with safety check of NSCs, adopting an approach based on q-factor (force reduction factor) to define inelastic FRS.
The influence of **damping** is generally similar, i.e., with increasing damping a reduction in FRS is observed. It is highlighted that this parameter is usually meant as an equivalent structural damping, aimed at representing the effect of hysteretic energy dissipation associated with NSC's response.
In a very recent study by Vukobratovic and Fajfar (2024) the influence of both factors is analysed, and previous literature studies are recalled.
Adam and Fotiu (2000) proposed two methods for generating the dynamic response of combined inelastic primary–secondary structures, without performing an eigenvalue analysis. The authors present the results of a parametric study on nonlinear SDOF NSCs in a supporting four-storey frame building, analysing the resulting displacement FRS. Villaverde (2006) analysed the nonlinear response of NSCs with an approximate method based on a procedure for the analysis of linear secondary systems mounted on a linear primary structure and the use of force reduction factors to account for the nonlinear behaviour of NSCs. Chaudhuri and Villaverde (2008) conducted an extensive parametric study on steel moment-resisting frames and both linear and nonlinear SDOF NSCs. The main finding regarding the influence of NSCs' nonlinear response was that the ductility demand on the NSC was generally lower than the assumed force reduction factor (ratio between elastic displacement demand and assumed displacement at yielding), i.e., the inelastic displacement demand was lower than the corresponding elastic value, except for NSCs with (initial) period close one of the higher modes' periods of the supporting structure and with the period in these modes lower than about 0.2 sec. Tamura et al. (2016) analysed the nonlinear response of NSCs constant-ductility FRS to reduce the required yield strength, assuming a ductility capacity value for the NSCs. The authors proposed simple formulations of the force reduction factor for nonlinear NSCs depending on period and ductility. Obando and Lopez-Garcia (2018) analysed the response of nonlinear NSCs supported by different types of structures (steel, RC-wall and RC-MRF, Moment Resisting Frame, buildings) responding linearly. The response of NSCs was assumed as bilinear perfectly elasto-plastic. Also in this study, force reduction factor values were assumed as the ratio between elastic displacement demand and assumed displacement at yielding. Results were analysed in terms of ratio

between inelastic and elastic displacement demand on the NSCs. The authors found that the equal displacement rule applied to periods higher than the characteristic period, assuming the latter as the fundamental period of the supporting structure instead of the characteristic period of the ground motion. Similarly, for periods lower than the characteristic period, the ratio between inelastic and elastic displacement demand on the NSCs increased with decreasing period, with local minima at the modal periods of the structure (lower resonance effect in nonlinear case rather than in linear case). The influence of damping was analysed as well, assuming a value of 0.02 instead of the initial value of 0.05 as damping ratio for the NSCs, finding significant differences only within tuning ranges (period of the NSC close to one of the natural periods of the supporting structure), where the ratio between inelastic and elastic displacement demand was lower for 0.02 than for 0.05 damping ratio (again, lower resonance effect in nonlinear case rather than in linear case).

Miranda et al. (2018) proposed an approach to the design of NSCs, highlighting that, very generally speaking, due to the narrow-band nature of elastic FRS, allowing a NSC to behave nonlinearly results in a significant decrease in acceleration demand especially in tuning conditions, even with a relatively limited ductility demand. In (Kazantzi et al., 2020a) the authors developed this approach, proposing force reduction factors for NSCs, based on the analysis of nonlinear NSCs subjected to floor motions from instrumented buildings in California, recorded mostly at the roof level but also at intermediate floors. In (Kazantzi et al., 2020b), the authors derived inelastic FRS with defined levels of ductility and two levels of damping (0.02 and 0.05 damping ratio). The results were in line with the main observations reported in the previous above-mentioned studies, with a reduction in acceleration that was especially beneficial in tuning conditions. With regard to the effect of damping, the authors observed that in the case of FRS this effect is significantly greater, again, in tuning conditions; this trend is qualitatively similar to the observed influence of nonlinearity in the response of NSC, with a remarkably greater beneficial effect (in this case, for a higher damping) in the case of tuning, that, as a matter of fact, produces the most detrimental effects when the response of the NSC is linear and the damping is lower.

Anajafi and Medina (2019) performed an extensive study on the influence of damping, starting from the numerical analysis of short-to-midrise US code-conforming steel moment resisting frame and RC shear wall buildings. Studying the response of NSCs with varying levels of damping ratio (from 0.01 to 0.09), the authors proposed a “damping modification factor” to modify FRS evaluated with a 0.05 damping ratio, in the case of higher or lower values of this ratio, providing simplifying formulations for this factor. The authors found that the greater effect of damping (of course, with increasing demand for decreasing damping ratio) was observed in tuning conditions. Anajafi et al. (2022) later validated the expressions proposed for “damping modification factor” in (Anajafi and Medina, 2019) based on recorded floor acceleration from instrumented buildings. Anajafi et al. (2020) investigated the influence of nonlinearity in the response of NSCs, analysing overstrength and ductility factors for nonlinear NSCs. The case study buildings were the same analysed in (Anajafi and Medina, 2019). In tuning conditions, the authors observed that nonlinearity was highly beneficial, resulting in a significant decrease of displacement demand. The highest beneficial effect for the NSC was observed in the case of tuning with the fundamental period of the supporting structure responding elastically, location on the roof and low damping. On the contrary, in non-tuning conditions, a detrimental effect of nonlinearity was observed, especially for rigid NSCs, with ductility demand higher than

overstrength, whereas for flexible NSCs the observed response is close to equal displacement rule, with ductility roughly equal to overstrength.

Di Domenico et al. (2021) analysed 3D numerical models of 2- to 8-storey Eurocode-conforming RC frames, designed for different levels of seismic intensity, from 0.05 to 0.35 g PGA at Life Safety Limit State, bare and uniformly infilled with a “weak” and a “strong” infill layout. The out-of-plane response of infill walls was explicitly modelled, with step-by-step consideration of in-plane/out-of-plane interaction effects, too. Then the authors proposed practical formulations for PFA/PGA profile and for FRS, the latter including two amplification (resonance) regions, one for the first mode and the other for higher modes, adopting as predictive parameters the floor height normalized with respect to the building height, the vibration periods, and the shape of the vibration modes of the building, the building height, and the PGA and the pseudo-spectral acceleration demands. The authors analysed the influence of NSCs’ damping ratio, too, ranging from 0.01 to 0.20, concluding that a very simple expression with the inverse of the damping ratio under square root, applied to the amplification factors for first and higher modes, could approximate well the observed trends.

Vukobratovic and Fajfar (2024) extended their previous proposal for FRS (Vukobratovic and Fajfar, 2017) accounting explicitly for nonlinearity in the response of NSCs. The authors analysed the influence of damping, too. After performing a parametric study with varying ductility and damping for the NSC, the authors concluded that nonlinearity and damping had a similar effect on the NSCs’ response, i.e., a negligible influence in the pre-resonance region and a beneficial effect in the resonance and post-resonance regions, and that the influence of damping was much more significant in the case of linear behaviour compared to nonlinear behaviour. The authors modified their original formulation introducing a NSC force reduction factor, explicitly applied in the off-resonance region (with a bilinear formulation depending on the NSC’s period and resulting in the application of equal displacement rule in the post-resonance region, and neglecting the effect of damping), and modifying the expression for the amplification factor in the resonance region (with two coefficients accounting for both nonlinearity and damping effects).

Magliulo and D’Angela (2024) analysed nonlinear SDOFs representative of NSCs consisting of cantilevers with hollow square steel sections with a mass at the free end, subjected to floor accelerograms recorded in RC buildings in US and to artificial accelerograms compliant with shake table protocols. The nonlinear response was modelled according to the Ibarra–Medina–Krawinkler approach (Ibarra et al., 2005), with response parameters calibrated by Lignos and Krawinkler (2010). The authors derived fragility curves at different Damage States and “component amplification factor” values (i.e., ratio between PSA and PFA). The latter, in particular, showed that nonlinearity in the response of NSCs led a decrease in acceleration demand, as much as PFA increased.

In conclusion, nonlinearity and damping have qualitatively similar effects on the response of NSCs. Studies on these topics are not yet many. However, they clearly and consistently point to the same conclusions. More specifically, as far as nonlinearity is concerned, its obvious effect is to “cut” the acceleration demand, but also another – not as obvious and very beneficial, that is, to decrease the displacement demand in the case of tuning (resonance), i.e., for NSCs with a period close to one of the supporting structure’s periods. In other terms, for nonlinear NSCs in the resonance region neither the equal energy rule ($\mu>R$) not the equal displacement rule ($\mu=R$) applies, but, on the contrary, the

ductility demand is lower than the overstrength (μ<R), and therefore the acceleration demand can be significantly reduced with respect to the elastic case even with a relatively limited ductility demand. A likely explanation of this effect comes from the nature of the floor accelerograms, as these signals differ from the ground accelerograms since they are filtered by the supporting structure. As a consequence, if a SDOF with a period within the narrow band of amplification (resonance region) experiences an even limited nonlinearity in the response, the consequent period elongation leads the response of the SDOF rapidly away from the peak of the resonance region, with a dramatic reduction in displacement demand. In the off-resonance regions, i.e., for a SDOF with a period outside this narrow band, nonlinearity effects are similar to what is observed for ground accelerograms, with an increase in displacement demand for rigid SDOFs (μ>R) and the applicability of equal displacement rule for flexible SDOFs (μ=R).

2.2.3 Interaction effects

FRS represent the dynamic response of the NSC subjected to the earthquake excitation "filtered" by the dynamic response of the supporting structure. Hence, if the latter is influenced by some effects, the FRS will be influenced, too. As well-known from several numerical and experimental studies, one of the most influential parameters for the dynamic response of the supporting structure is the presence of masonry **infill walls**, especially for RC frame buildings. Another type of possible dynamic interaction is the one **between the supporting structure and the NSC itself**. Usually, this effect is deemed as negligible, due to the much smaller mass of the NSC compared to the structure, but in some cases it can become significant. These interactions and their possible effects will be discussed in the following.

Mollaioli et al. (2010) investigated the influence of the presence of infill walls on FRS analysing planar numerical models of RC frames, representative of existing buildings, with different number of storeys (from 2 to 10) and different infills' layout ("bare" model – without infills, uniformly infilled model and "pilotis" model – with open ground storey). Based on their analysis, the authors concluded that infills led to a significant change in the shape of FRS, but not in the shape of peak floor acceleration (PFA) along building height. The change in the shape of FRS consisted of the presence of a plateau – rather than a peak – of amplification between the first and second building's period. Moreover, a shift of the period(s) corresponding to maximum amplification was observed, due to the period elongation affecting buildings with infills because of the damage to these elements. In (Lucchini et al., 2014), the authors analysed planar numerical models of 4- and 6-storey RC frames, representative of existing buildings, bare and uniformly infilled, observing that the change in the PFA profile due to infills' presence was not negligible, i.e., up to -20%/+40% compared to bare buildings, and that in FRS the presence of infills led to a broader, less concentrated range of amplification, with generally lower peak values. A reduction in these effects were observed for higher seismic intensity, that is, with more damaged infills. Asgarian and McClure (2014) analysed the response of a case-study hospital RC building, with and without infill walls, with a detailed numerical model validated on the dynamic response of the real building measured through ambient vibration tests, prior to and after the construction of infill walls. They observed that the presence of infills led to a shift in the peak of FRS

due to the reduction in the vibration period of the structure, potentially detrimental for NSCs, especially at upper storeys. Blasi et al. (2018) analysed the response of planar numerical models of 4- to 10-storey RC frames, representative of existing buildings, bare and uniformly infilled. Also in this case, the authors observed a shift in the peaks of the FRS due to the decrease in the natural periods of the supporting structure, and a relatively lower contribution of higher modes, attributable to a beneficial increase in the regularity in elevation caused by infills' presence. Surana et al. (2018a), based on the numerical analysis of 2- to 12-storey RC frames designed for seismic loads according to Indian technical codes, proposed a "floor amplification function" for inelastic RC frames without infills, to estimate the floor response spectrum directly from the ground response spectrum; this function was made of a central parabolic part capturing the amplification related to first and second mode. In Surana et al. (2018b) the authors extended their proposal to RC buildings with infills, analysing 4- and 8-storey uniformly infilled and pilotis RC frames. The authors observed that the effect of period elongation, and consequent shift of the amplification peak, was much more significant when infills were present, due to their damage evolution compared to RC structural members. Finally, they proposed a modified "floor amplification function" for infilled frames with two parabolic parts capturing separately the amplification effects related to first and second mode. In (Di Domenico et al., 2021) (see Section 2.2.2) the main observations drawn by the authors regarding infill walls were that these elements led to an increase in maximum PFA and PSA, especially for mid- and high-rise buildings, and, in these buildings, they further increased the amplification effects related to higher vibration modes that led to significant acceleration demand also at medium-low storeys.

In summary, the main influence of infill walls on FRS seems to consist of a variation in the modal properties of the supporting structure, due to the stiffening contribution of these elements, that leads to a variation in the periods associated with maximum amplification and possibly to a change in the shape of the FRS amplification range; then, the damage to these elements – that leads to a particularly rapid stiffness decrease – leads, in nonlinear field, to shift of the above-mentioned amplification peaks.

One of the earliest studies about the dynamic interaction between the supporting structure and the NSC (or the "secondary" structure) was published by Sackman and Kelly (1979). The authors developed an analytical method specifically for the case of tuning between the supporting structure and the NSC, which led to a significant dynamic interaction not accounted for by conventional FRS. The authors observed that the significance of this dynamic interaction decreased with decreasing component-to-structure mass ratio and with increasing component damping ratio. This approach was extended to the non-tuning case as well. Igusa and Der Kiureghian (1985a,1985b) highlighted that the classical FRS approach, neglecting the dynamic interaction between the primary and the secondary structure, can lead to very significant errors, usually on the conservative side, especially in the tuning case, also due to statistical assumptions that neglected cross-correlations between support motions and between modal responses. In this study, the authors proposed a method for the dynamic analysis of composite primary-secondary structural systems accounting for the effects of tuning, interaction, nonclassical damping, and spatial coupling. The method consisted of (i) the synthesis of the modal properties of the composite system starting from the properties of the primary

and secondary structures and (ii) the modal analysis of the composite system. In (Igusa and Der Kiureghian, 1985c), the authors developed the method proposed previously, specializing it to the common case of secondary system represented by a SDOF with a single attachment point to the primary structure and applying it to the generation of FRS. The authors highlighted that the interaction phenomenon generally reduces the response of the secondary structure, particularly when there is tuning and the secondary mass is not too small (i.e., at least 0.0001 times the mass of the primary structure). This method was further developed in (Asfura and Der Kiureghian, 1986). A similar approach was later developed by Suarez and Singh (1987), providing FRS accounting for dynamic interaction starting from the modal properties of the primary and secondary structures, also using as seismic input smoothed ground response spectra. A description of this type of approaches can be found in (Chen and Soong, 1988). Chen and Wu (1999) proposed criteria to define situations in which a decoupled analysis of primary and secondary structure was acceptable. Both SDOF and MDOF primary structures were considered. These criteria consisted of an upper bound secondary-to-primary mass ratio, and an interval of secondary-to-primary frequency ratio; these limits were a function of the accepted tolerance error due to neglecting coupling effects. Below the mass ratio upper bound and outside the frequency ratio interval a coupled analysis was deemed not necessary.

Taghavi and Miranda (2008) analysed the interaction effects between the primary and the secondary structure starting from the transfer function approach proposed by Gupta (1997), in which the dynamic interaction between the primary and the secondary structure is first neglected, and then accounted for by applying to the primary structure the interaction force between the two structures. The authors adopted the continuum modeling approach proposed in (Miranda and Taghavi, 2005) to estimate the dynamic characteristics of the primary structure. Then, they performed a parametric study analysing the effect of fundamental period of the primary structure, lateral stiffness ratio of the primary structure (ratio between lateral stiffness at the top and lateral stiffness at the base of the primary structure), damping ratio of the primary and secondary structures, and secondary-to-primary mass ratio. The authors observed that, in the case of tuning between primary and secondary structure, the response of the primary structure was significantly affected by dynamic interaction with the secondary structure if the frequency of the input motion was around the frequency of the secondary structure and the mass ratio was at least equal to 0.1; the result of this interaction was a decrease in the transfer function values. Similarly, the acceleration transfer function of the secondary structure showed a marked decrease if the frequency of the input motion was around the frequency of the secondary structure and the mass ratio was at least equal to 0.1. Then, the authors also analysed FRS, observing that coupling effects had a non-negligible influence, consisting of a decrease in acceleration demand, if the mass ratio was at least equal to 0.01 and the period was close to the modal periods of the primary structure. For a mass ratio equal to 0.1, such a decrease was very significant and noticeable also between modal periods. The authors observed that these interaction effects increased with decreasing damping ratio of the secondary structure. Adam and Furtmüller (2008a) analysed the supporting structure and the NSC as two springs in series, the former elasto-plastic, and the latter linear elastic. The authors derived constant ductility acceleration and displacement floor spectra and performed uncoupled analyses, too, thus directly observing the influence of dynamic interaction. More specifically, the comparison between displacement floor spectra evaluated in the hypotheses of coupling and decoupling showed that neglecting the coupling effect led to a significant, excessively

conservative overestimation in the tuning case – especially for high NSC mass, to a lower but still significant overestimation for NSC period higher than supporting structure's period, and vice versa to a non-conservative underestimation for NSC period lower than supporting structure's period; with increasing ductility, generally, the overestimation decreased and the underestimation increased. In (Adam and Furtmüller, 2008b) the authors extended their approach adopting an inelastic MDOF instead of an SDOF as supporting structure, and they observed that the SDOF simplification generally yielded a quite accurate approximation. (Adam et al., 2013) derived FRS for moderately heavy NSCs attached to elastic and inelastic SDOF and MDOF supporting structures, and then proposed a simplified, approximate method to derive FRS for in the case of MDOF supporting structures with a modal decomposition approach. Assuming a 0.05 mass ratio between the mass of the NSC and the effective modal mass associated to the first mode of the MDOF supporting structure, the authors observed that with an elastic supporting structure neglecting the coupling effects could lead, in the tuning case, to very conservative results, with more that 100% overestimation of displacement and acceleration demand. Again, inelasticity in the response of the MDOF supporting structure lowered this overestimation. Lim and Chouw (2014) analysed the interaction between primary and secondary structures through experimental shake table tests with both SDOF structures, with different types of excitations, corresponding to soft, medium, or hard soil. The authors observed a varying influence of this interaction on the response of the primary structure, depending on the type of excitation. In (Lim and Chouw, 2018) the authors carried out further shake table tests on primary and secondary interacting SDOF structures subjected to impact and harmonic loads, varying the stiffness of the connection between the two. The authors observed an increase in the acceleration demand on the secondary structure with increasing stiffness of the connection, and vice versa for the displacement demand; they also proposed empirical formulations to predict the displacement demand on the secondary structure depending on the displacement demand at its support and the stiffness of the connection. Vela et al. (2018, 2019) derived FRS for a special concentrically braced frame supporting a cylindrical storage tank. To investigate the effect of coupling, the authors ran analyses with and without the secondary structure and compared the resulting FRS, also evaluating the influence of damping of the secondary structure. The authors observed that in the resonance region with the fundamental period of the primary structure neglecting the interaction effects led to a significant overestimation of the acceleration demand, especially for lower damping and at higher seismic intensities.

In conclusion, the study of dynamic interaction between a primary (supporting) structure and a secondary (supported) structure – or NSC – was first based on the development of refined analytical methods for the analysis of the modal response of systems in series, accounting for the typical phenomena characterizing interacting systems, that is, tuning, dynamic interaction, and non-classical damping. The main observations drawn from these studies were that the most significant consequence of neglecting the dynamic interaction was a significant and overly conservative overestimation of the demand on the secondary structure, observed in case of tuning and non-negligible secondary-to-primary mass ratio. In the following years, further, parametric and generally less mathematically rigorous studies were focused on this topic, also investigating the influence of a

possible inelastic response of the primary and/or secondary structure, generally concluding the interaction effects were more significant in elastic field.

2.2.4 Effects of the characteristics of the ground motion excitation

Seismic demand on NSCs in terms of FRS is primarily related, of course, to the input ground motion excitation. In this regard, some specific aspects deserve a more accurate discussion, that is, the effects of the **vertical component** of the ground motion, and the possible presence of a **near-fault** ground motion.

Most of the studies on the structural amplification of the vertical component are relatively recent. Swanson et al. (2012) analysed the critical issue of earthquake effects on computer equipment supported by raised access floors in data processing facilities. The authors analysed a case-study three-story frame steel building, concluding that current code-based FRS were unconservative, underestimating the vertical component of the seismic demand on NSCs. Qu et al. (2014) analysed ASCE code provisions for seismic demand on NSCs based on data recorded on RC shear wall, steel MRF and steel braced buildings, from low-rise to high-rise, and from moderate to severe earthquakes. Again, also in this case the authors observed that code assumptions – namely, constant instead of increasing along the height vertical PFA distribution – was unrealistic and unconservative. Furthermore, the authors observed that the shape of vertical FRS was very similar along the height of the buildings, and that the highest demand occurred in case of tuning between the NSC and the structure in vertical direction. Moschen et al. (2015, 2016) analysed the seismic demand in vertical direction along column lines of elastic steel MRF buildings, with number of storeys between 1 and 20, designed based on older and modern US codes. To this end, dynamic analyses were performed on simplified stick models representative of the perimeter frames, also considering two different damping ratios (0.02 and 0.05). The authors observed that vertical PFAs were much larger (up to three times) than the vertical PGA (that, in turn, can be assumed as 2/3 of the horizontal PGA) and increased with height, and they finally proposed a simplified expression providing the vertical PFA as a function of the horizontal PGA, of the height within the building, and of the damping ratio. Gremer et al. (2018, 2019) analysed horizontal and vertical PFAs in two-dimensional steel MRFs, with number of storeys between 1 and 20, based on FEMA P-695 (2009) archetype structures. The authors analysed the acceleration demand also away from column lines, i.e., along horizontal beams. They analysed the influence of different parameters, including a modified beams' stiffness (representing the effect provided by the presence of the floor slab on the beam flexural stiffness), a modified mass distribution (masses equally distributed over all nodes instead of larger masses – due to larger tributary areas – in nodes closer to exterior column lines), and a modified damping ratio (from 0.01 to 0.08). The authors found that maximum vertical PFAs (at the top of the buildings) were about two to five times the vertical PGA, with higher values for taller frames, and that vertical PFAs increased along the height. The flexural deformability of beams led to an increase in vertical PFAs, with higher values away from column lines. This amplification effect increased with a uniform mass distribution but was not significantly affected by the increase in beams' stiffness. Finally, the effect of damping (i.e., PFA decrease with increasing damping ratio) was similar in horizontal and vertical direction. Francis et al. (2017) performed nonlinear dynamic analyses on a four-storey two-dimensional building model

representing an RC shear wall building in New Zealand, analysing vertical acceleration demands at the mid-section of the wall and mid-span of the beam element at the first and top floor levels. The authors observed that the maximum spectral vertical acceleration demand on the roof storey beam was more than 7 times the vertical PGA, attained for a period slightly higher than 0.2 s. Reducing the inertia of the beam elements, in order to resemble the inertia of a typical hollow core floor slab, the authors observed the absence of a peak in spectral vertical acceleration. Also, the authors investigated the effect of a damping ratio equal to 0.02 or 0.05, observing, as expected, a reduction in acceleration demand with increasing damping. (Ryan et al., 2016; Soroushian et al., 2016) the experimental results of a shake table test on a full-scale five-story steel MRF building in base-isolated and fixed-base configurations are analysed. Regarding vertical acceleration demand, the authors observed that the vertical PFA at column lines was approximately between 2 and 3 times the peak vertical acceleration of the table, without a significant dependence on the height. The vertical PFA in the middle of floor slabs was significantly higher, i.e., approximately from 3 to 6 times the peak vertical acceleration of the table, due to local amplification. Specifically, a lower and constant over height amplification was observed in slabs with lower period and larger damping ratios, roughly constant over height, whereas a higher and increasing with height amplification was observed in slabs with period increasing with height and damping ratio decreasing with height. Starting from the observation of these experimental results, Guzman Pujols and Ryan (2020) carried out a numerical study focusing their attention on the slab amplification effects. The case study building was a three-storey steel braced frame, in base-isolated and fixed-base configurations. The effects of additional mass on slabs, irregularly distributed, were investigated as well. The average vertical spectral acceleration in slabs was found to be approximately 2.5 to 6.5 times the vertical PGA. However, the authors concluded that added floor mass, vertical isolation period in the base-isolated building, and slab flexibility had no significant/systematic effect on slab amplification.

In summary, literature studies consistently indicate that neglecting amplification of vertical accelerations, usually increasing with height, can result in a significantly unconservative underestimation of vertical acceleration demand on NSCs. Moreover, in RC and steel buildings further significant, local amplification effects are observed away from column/wall lines, i.e., in the middle of floor slabs, due to the out-of-plane flexural deformability of these elements.

Sankaranarayanan and Medina (2006) analysed structures representing “stiff” and “flexible” MRFs with number of storeys between 3 and 18, subjected to the pulse-like fault-normal component of near-field ground motions. MRFs with different strength, thereby responding elastically or inelastically, were analysed. The authors observed that the ratio between the peak acceleration of a NSC mounted on an elastic frame to that of a NSC mounted on an inelastic frame was not significantly different from the case of ordinary ground motions, concluding that no specific design procedure was probably necessary in the near-field case. A very similar approach was later followed by Kanee et al. (2013), reaching very similar conclusions. Alonso-Rodríguez and Miranda (2015) developed a simplified approach to derive closed-form solutions for acceleration and drift response along height of buildings subjected to near-fault pulse-like ground motions, in elastic field. To this aim, the authors started from the study by Mavroeidis and Papageorgiou (2003), that proposed a pulse model, i.e., the expression

of an acceleration time history representing a near-fault pulse-like ground motion, depending on some input parameters including the amplitude and the predominant frequency of the pulse. Mavroeidis et al. (2004) derived a closed-form solution for the response of an undamped SDOF system subjected to such an input. The authors derived a closed-form solution for the case of a damped SDOF system, too, and then adopted the simplified approach proposed in (Miranda and Taghavi, 2005) to represent multi-storey buildings with a continuous flexural/shear beam coupled model, finally deriving closed-form expressions for acceleration and drift response profiles. The authors checked the validity of this approximated approach comparing these results to the results of dynamic analyses of the adopted simplified continuous model subjected to "true" pulse-like near-fault ground motions. With their simplified approach, the authors then performed a parametric analysis, mainly observing that higher values of PFA along height were obtained if the predominant pulse period approached the first mode period, and that, if the predominant pulse period was equal to the first mode period, PFA increased almost proportionally with pulse duration. Zhai et al. (2016) and Pan et al. (2017) investigated the effects of near-fault pulse-like ground motions on the seismic demand on NSCs performing nonlinear dynamic analyses of a SDOF system representing the primary structure under 81 near-fault pulse-like ground motions and 573 non-pulse-like ground motions, varying the ductility demand on the primary structure (between 2 and 6), the damping ratio of the NSC (from 0.01 to 0.20), and assuming three different hysteretic response models for the primary structure. Then, the authors derived FRS for these cases and for the case of elastic primary structure and calculated the "amplification factors" as ratios between FRS for an inelastic primary structure and FRS for an elastic primary structure, reporting them as a function of the NSC-to-primary structure period ratio. Amplification factors were generally lower than 1, especially in the case of tuning, i.e. when NSC-to-primary structure period ratio was close to 1, indicating the beneficial effect of nonlinearity of the primary structure's response; this beneficial effect increased with increasing ductility. Compared to ordinary ground motions, significant differences were observed in the case of tuning, with higher amplification factors for near-fault ground motions, especially for higher ductility. Within the near-fault ground motions dataset, amplification factors were observed to increase with magnitude, whereas no clear and systematically beneficial or detrimental effect of rupture distance, Peak Ground Velocity and Maximum Incremental Velocity were observed. Regarding the hysteretic response models for the primary structure, a degrading response led to lower amplification factors for ordinary ground motions (especially in the tuning case), likely because response degradation of the primary structure (that is beneficial for the seismic demand on NSCs) is more significant for ordinary ground motions. With increasing damping ratio of the NSC, amplification factors decreased, i.e., FRS for inelastic and elastic primary structure were closer. Finally, the authors proposed a formulation predicting amplification factors for near-fault pulse-like ground motions, as a function of the NSC-to-primary structure period ratio and the ductility demand on the primary structure.

If the rupture front propagates toward the site of the building and the direction of slip on the fault is aligned with the site, forward rupture directivity effects can occur, with the fault-normal component of the ground motion presenting a high-energy velocity pulse at the beginning of the record (Somerville et al., 1997); this is the case of "near-fault pulse-like ground motions". These characteristics of the ground motion can affect the seismic demand on NSCs. Few specific studies have addressed this

issue so far. In summary, the main conclusions drawn from these studies highlight that, under a near-fault pulse-like ground motion, if the primary structure remains elastic, the PFA can be higher than in the case of ordinary ground motions, especially if the predominant pulse period approaches the first mode period of the primary structure, and, in this case, if the pulse duration is higher. If the primary structure responds inelastically, the ratio between “inelastic” and “elastic” FRS ordinates is higher than in the case of ordinary ground motions, especially if the NSC period approaches the first mode period of the primary structure.

2.2.5 Summary of the effects induced on FRS by the examined influencing parameters

Table **2** summarizes the main effects on FRS induced by the influencing parameters examined in Sections 2.2.1, 2.2.2, 2.2.3, 2.2.4.

Table 2. Summary of the main effects induced by the examined influencing parameters on FRS.

Factors	**Influencing parameter**	**Main effect**	**Relevant bibliography**
Supporting structure	Dynamic response	Filters the ground motion at the predominant frequencies of vibrations of the building	• Landge and Ingle 2021 • Menon and Magenes 2011a-b
	Nonlinear behaviour	Usually decreases FRS	• Kingston 2004 • Rodriguez et al. 2002
		Sometimes increases FRS (non-tuned NSCs in buildings with localized plasticity)	• Anajafi 2018 • Chaudhuri and Villaverde 2008
		Primarily affects the first mode	• Kingston 2004 • Rodriguez et al. 2002
	In-plane diaphragm flexibility	Introduces degrees of freedom, potentially adding higher modes	• Anajafi and Medina 2019
		Increases the building modal periods with detrimental or beneficial global effects depending on the period of the building with a rigid diaphragm assumption and the ground motion frequency content	• Tena-Colunga et al. 2015
		Amplifies PFA responses at the center of the diaphragm with respect to edges	• Ruggieri and Vukobratovic 2023 • Derakhshan et al. 2022
	Torsional response	Together with diaphragm flexibility, amplifies PFA responses	• Qu et al. 2014
		Amplifies the floor acceleration responses	• Jain and Surana 2022 • Landge and Ingle 2022, 2021
NSC	Nonlinear behaviour	Obviously decreases the acceleration demand but, in case of tuning, also decreases the displacement demand, with a ductility demand lower than the overstrength (μ<R)	• Kazantzi et al. 2020b • Vukobratovic and Fajfar 2024
	Damping	An increase in damping has qualitatively similar effects to an increase in nonlinearity of the response	• Kazantzi et al. 2020b • Vukobratovic and Fajfar 2024
Interaction	Interaction with infills	Changes in the shape of the FRS amplification range due to the infill stiffness contribution	• Di Domenico et al. 2021 • Lucchini et al. 2014
	Interaction with NSCs	Neglecting the dynamic interaction overestimates the demand on NSCs, in case of tuning and non-negligible secondary-to-primary mass ratio	• Igusa and Der Kiureghian 1985a-b
Ground motion excitation	Vertical component	Neglecting the vertical component of the ground motion underestimates the demand on NSCs	• Gremer et al. 2019 • Moschen et al. 2016, 2015
	Near-fault pulse-like ground motion	Increasing of PFA especially for pulse periods approaching the fundamental period of the primary structure (in elastic field) Increasing of the ratio between “inelastic” and “elastic” FRS especially for NSC period approaching the fundamental period of the primary structure (in nonlinear field)	• Pan et al. 2017 • Zhai et al. 2016 • Mavroeidis et al. 2004

2.3 Past experimental studies

This Section summarizes the outcomes of the review of past experimental shake-table tests performed in the recent past to assess the seismic demands on NSCs. The review was conducted to recon the amount and nature of these experimental campaigns, and to summarize related research results. The methodology applied constitutes of the following steps: 1) searching on the Scopus database for relevant experimental studies; 2) selecting studies based on pre-defined inclusion criteria; 3) collecting, summarizing, and reporting the main characteristics of the tested prototype and of the test set-up, the investigated parameters, and the main results.

A first corpus of experimental shake-table campaigns described in research papers were built searching on the Scopus database through relevant keywords (floor response spectrum OR floor response spectra AND shake-table tests OR shaking table tests). The result was 39 documents dating from 1980 to 2024. Then, the research was limited to the subject area (i.e., “engineering”), the document type (only journal and review papers were selected), and language (i.e., “English”). From this selection, 25 documents have remained. Finally, the non-relevant articles were excluded to further refine the results and come to the final corpus of research papers to be reviewed. Only the experimental campaigns whose aim was to assess the acceleration demands on NSCs performed in the recent past were selected, in coherence with the purpose of WP1 (for example, tests addressed to the characterization of the seismic performance of the NSC only were excluded). The final corpus of papers to review was 17 documents from 2010 to 2024. They are presented in Table 3, together with the number of tested specimens and the parameters investigated in each shake-table campaign. From these papers, the information summarized in Table 4 was extracted and collected in an Excel database attached to this Deliverable. They can be grouped into three main categories: data about the reference (highlighted in green in Table 4), experimental data on prototype and set-up (in light blue), and main results achieved and observed trends (in pink). More in detail, the database includes, for each experimental campaign, prototype features (*e.g.,* scale, number of tested specimens, material, number of stories, diaphragm typology, examined configurations, and main geometrical data), test set-up (*e.g.,* test program, instrumentation, excitation application), results (specifying the availability of dynamic identification tests, experimental figures of damage, force-displacement response of the specimen, PFA profiles, floor accelerations and FRS), and investigated parameters and main observed trends (*e.g.,* aims of the experimental campaign and main outcomes). The sources are clarified, specifying the whole reference, and providing the link of Scopus when available for the download. Furthermore, for each source, it is specified if the results are available, not available, or available only on request for further elaboration.

Table 3. List of references included in the experimental database, number of tested specimens, and parameters investigated in each shake-table campaign.

Reference	N° of specimens	Investigated parameters
Xiao et al. 2024	1	Effect of modelling assumptions on the dynamic behaviour of a short-period RC shear wall structure on acceleration time-histories and FRS
Wu et al. 2024	1	• Seismic performance of water supply pipes installed in a full-scale sample (RC) • Effect of different material pipes and different methods for penetrating the RC floors
Wu et al. 2022	1	• Seismic performance of water supply pipes installed in a full-scale sample (masonry) • Effect of different material pipes and different methods for penetrating the RC floors
Xiaoguang et al. 2023	1	• Correlation between NSC dynamic amplification factor and building dynamic characteristics and relative height • Correlation of FRS peaks with floor level and damping rations of NSCs
Yuande et al. 2023	2	Effectiveness of seismic isolation by friction pendulum bearings (FPBs) in protecting structural and non-structural components
Butenweg et al. 2021	1	Interaction between primary and secondary elements in an industrial structure equipped with complex process components
Vukobratović et al. 2021	3	• Prototype nonlinearity • Influence of the building fundamental period on PFA/PGA • “Elongated Fundamental Mode Effect” • Energy distribution in the “Elongated • Fundamental Mode Effect”
Crozet et al. 2019	1	Effect of pounding between adjacent structures induced by earthquakes on equipment and on the structures themselves
Chakraborty et al. 2017	1	Energy-transfer phenomenon
Kothari et al. 2017	1	Prototype nonlinearity
Zhang et al. 2016 Zhang et al. 2017	1	Equipment-structure-soil (ESS) interaction
Ryan et al. 2016	1	Seismic response of a steel building with an integrated suspended ceiling-partition wall-sprinkler piping system in base-isolated and fixed-base configurations
Beyer et al. 2015	1	Prototype nonlinearity
Lepage et al. 2012	30	Prototype nonlinearity
Tashkov et al. 2010	1	Effectiveness of a floating sliding base-isolation system
Bothara et al. 2010	1	Prototype nonlinearity

Table 4. Summary of the information extracted from the selected papers and collected in an Excel database.

Sources	• Authors, Title, Years, Journal and Publication data • Abstract, Keywords • Link Scopus (when available)
Prototype features	• Scale • Number of the examined specimens • Lateral resisting system (LRS) • Materials of the LRS (RC: reinforced concrete; URM: unreinforced masonry; S: steel; Mixed) • Number of stories • Diaphragm typology → then, it can be classified in stiff or flexible • Geometric data (plan dimension and interstory height in [m]) • Prototype configurations (e.g., fixed base and with seismic isolation, as-built vs strengthened configurations,…)

Test set-up	• Test program and ground motion
	  ○ number of tests, number, and characteristics of ground motion,
	  ○ Range of PGA of the records used
	• Instrumentation (e.g., sensors type and distribution)
	• Excitation application (unidirectional, bidirectional, three directional)

Results	• Availability of dynamic identification of the prototype • Availability of experimental figures of damage • Availability of Force-Displacement response of the prototype • Availability of PFA profiles • Availability of floor accelerations • Availability of floor response spectra
Data availability	If “Available”, “Not Available”, and “Available on request”.
Investigated parameters and observed trends	• Objective of the experimental tests / investigated parameters • Observed trend

As it is possible to see from Figure 4, most of the experimental shake-table campaign included into the database tested reinforced concrete or steel specimens, built in a reduced scale, typically characterized by more than one story and with rigid diaphragms. In one case (Tashkov et al. 2010), a 1:3.5 prototype of a church was tested. All the examined experimental campaign tested only one prototype (Table 3), except for Yuande et al. 2023 (where two RC frame specimens were tested in the base-isolated and non-isolated configurations), Vukobratović et al. 2021 (who reported and discussed the tests on three reinforced concrete buildings tested at the E-Defense testing facility), and Lepage et al. 2012 (who discussed the results of an experimental campaign on 30 small-scale reinforced concrete structures). Furthermore, the same experimental campaign was discussed in Zhang et al. 2016 and Zhang et al. 2017. Figure 5 illustrates some pictures of the tested prototypes.

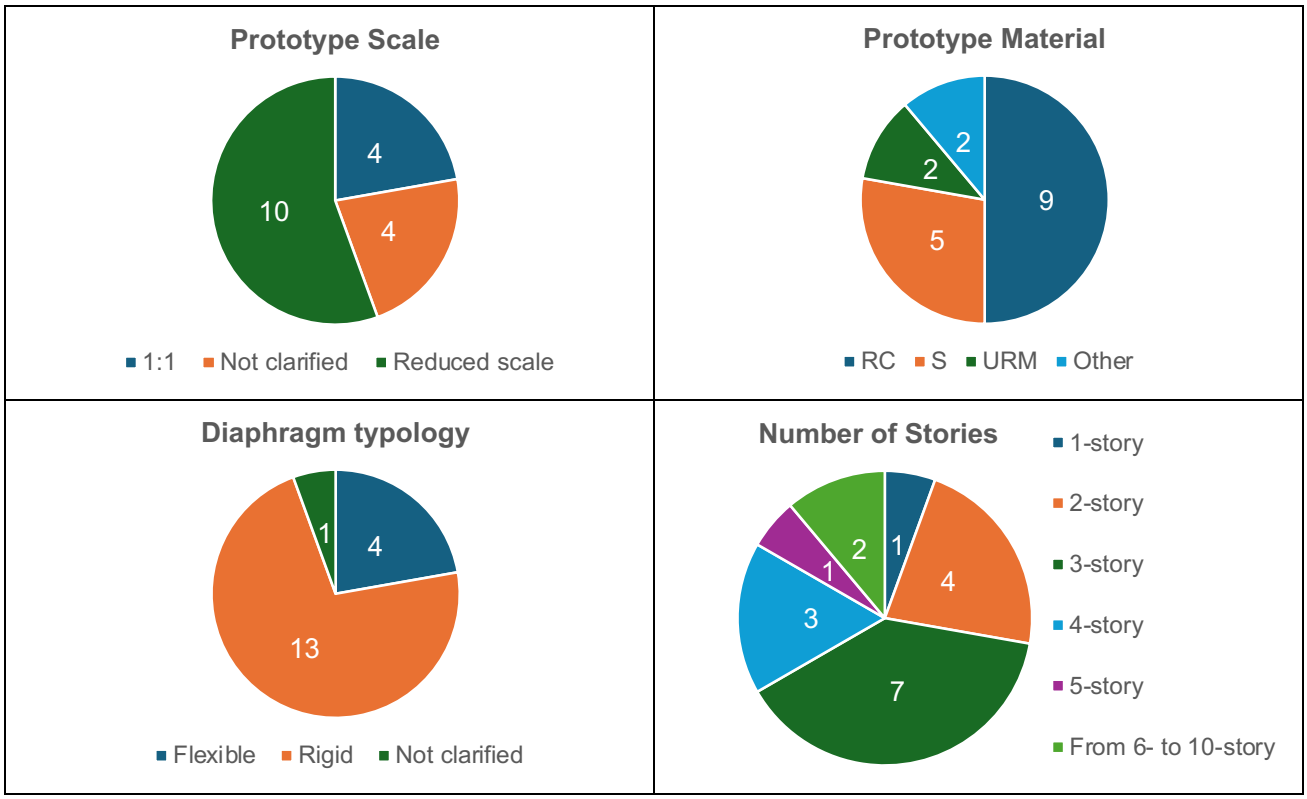

Figure 4. Summary of the main features of the experimental campaign reviewed.

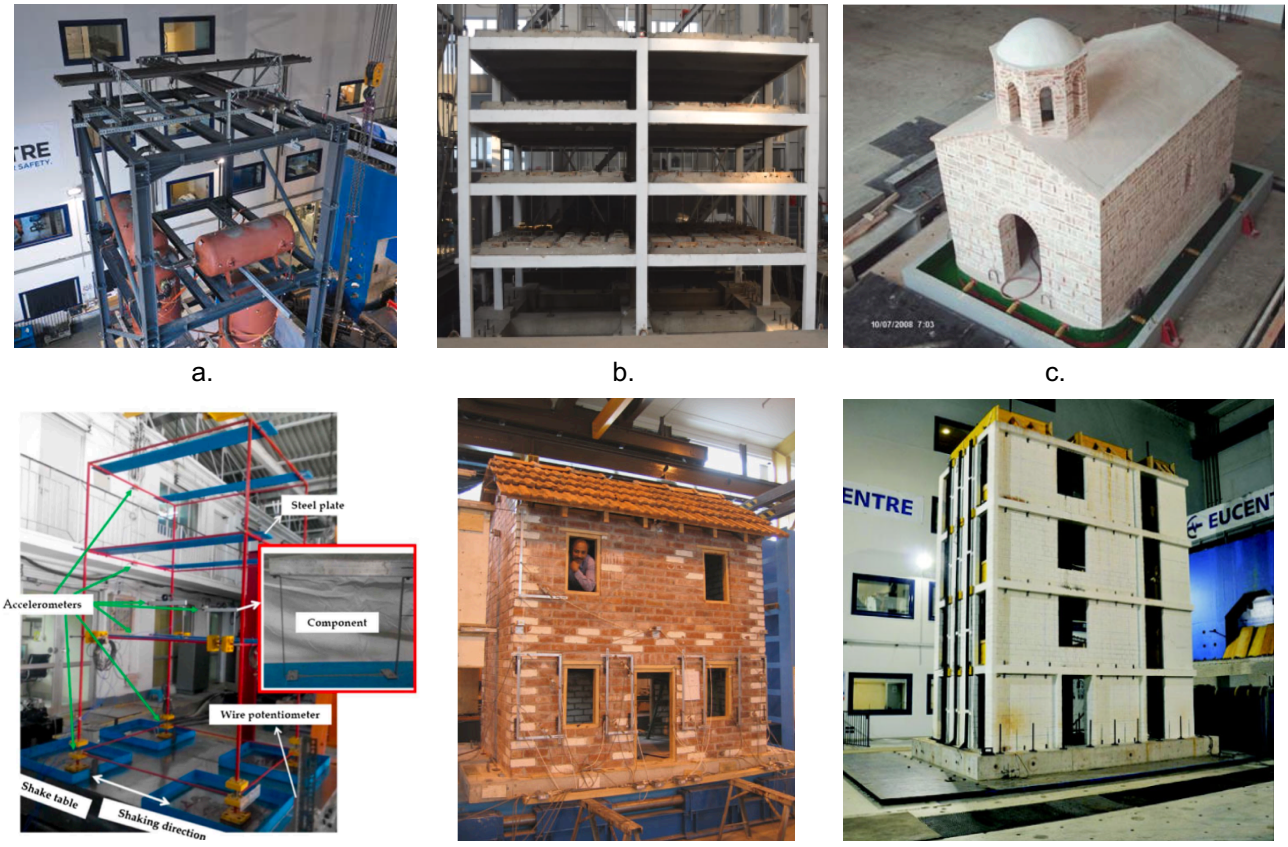

a. b. c.

d. e. f.

Figure 5. Pictures of the specimens tested in some campaigns included in the database: a. Butenweg et al. 2021; b. Yuande et al. 2023; c. Tashkov et al. 2010; d. Chakraborty et al. 2017; e. Bothara et al. 2010; f. Beyer et al. 2015.

The main objectives of the examined experimental campaign are reported in Table 3, while for all the other details it is possible to refer to the attached database which also reports a summary of the main experimental outcomes.

3 Review of code methods for the computation of the NSCs seismic demand

This Section presents the comparison of some code proposals, *i.e.* the proposal included in Section 4.3.5 of the Eurocode 8, the proposal included in ASCE/SEI 7-10 in Section 13.3.1, the proposal of the New Zealand code NZSEE2017 in section C7.6.2, and the three proposals included in Section 7.2.3 of the Commentary of the current Italian building code (Circolare 2019).

Eurocode 8 in Section 4.3.5 proposes the expression reported in Eq. (1) for the FRS evaluation whose theoretical derivation is not clearly stated. This proposal will be defined as EC8 hereinafter. In Eq. (1), T_a is the fundamental period of the nonstructural element, T_1 is the fundamental period of the building in the relevant direction, PGA is the peak ground acceleration, Z is the height of the nonstructural element above the level of application of the seismic action and H is the building height.
It is worth noting that if T_a=0, a linear PFA distribution along the building height is obtained varying the Z/H ratio. It can be noticed that PFA ranges from PGA (when Z=0) to 2.5PGA (when Z/H=1), while the maximum peak spectral acceleration is always obtained when $T=T_1$. If T equals T_1, the maximum peak spectral acceleration ranges from 2.5PGA (if Z=0) to 5.5PGA (if Z=H). It is interesting to observe that this expression does not include the effect of damping features (neither the damping of the nonstructural element, nor the one of the building); thus, it is impossible to quantify the effects of nonlinearity with this expression. Furthermore, it only allows considering the various position of the secondary element along the building height, while it makes impossible to consider torsional effects or effects due to diaphragm flexibility associated to a different position of the element in plan.

$$S_{a,Z}(T_a) = \mathrm{PGA}\left[\frac{3(1+\mathrm{Z/H})}{1+(1-\mathrm{T_a/T_1})^2}-0.5\right] \geq \mathrm{PGA} \quad (1)$$

ASCE/SEI 7-10 (in Section 13.3.1) proposed Eq. (2) for the Peak Spectral Acceleration (PSA). This proposal will be defined as ASCE/SEI 7-10 hereinafter. In the equation, a_p is a factor accounting for the amplification of acceleration due to the deformability of the nonstructural element reported in Table 13.5-1 of the code. It is worth noting that the American approach, with this factor, simplifies the calculation of the seismic demand acting on a NSC, as there is no need of a more or less detailed dynamic characterization to determine its period, T_a, which enters EC8 formulation.
Also, according to the ASCE/SEI 7-10 approach, the PFA varies linearly along the building height. It ranges from PGA (at Z equal to zero) to 3PGA (at Z equal to H). The maximum value of a_p reported in Table 13.5-1 of the code is equal to 2.5. Hence, the maximum possible PSA value is always equal to 2.5PFA, independently on the floor considered.

$$S_{a,Z} = \mathrm{PGA}\left(1 + 2\frac{\mathrm{Z}}{\mathrm{H}}\right)\mathrm{a_p} \tag{2}$$

The New Zealand code NZSEE2017, in section C7.6.2, refers to the loading code NZS 1170.5 for the calculation of FRS. NZS 1170.5, in Section 8.5.1, provides the formulation reported in Eq. (3).

$$S_{a,Z}(T_a) = \mathrm{PGA}\,\mathrm{C_{Hi}}\,\mathrm{C_i}(\mathrm{T_a}) \tag{3}$$

C_{Hi} is the floor acceleration coefficient at level i and it is calculated through the formulations reported in Eq. (4) and defines the PFA distribution along the building height which is, in this case, multilinear. The PFA ranges from PGA (at Z equal to zero) to 3PGA (at Z equal to H).

$$\mathrm{C}_{Hi} = \begin{cases} 1 + \dfrac{\mathrm{Z}}{6}, & for\ Z < 12m \\ 1 + 10\dfrac{\mathrm{Z}}{H}, & for\ Z < 0.2H \\ 3, & for\ Z \geq 0.2H \end{cases} \tag{4}$$

In Eq. (3), $C_i(T_a)$ is the spectral shape coefficient. $C_i(T_a)$ is expressed as a function of the period T_a as illustrated in Eq. (5) according to the new version of the NZSEE2017 (Section C8.10.3):

$$C_i(T_a) = \begin{cases} 2, & for\ T_a \leq 0.5\ s \\ 2\left(\dfrac{0.5}{T_a}\right)^{0.75}, & for\ 0.5\ s < T_a < 1.5\ s \\ 1.32/T_a, & for\ 1.5\ s < T_a < 3\ s \\ 3.96/{T_a}^2, & for\ T_a \geq 3\ s \end{cases} \tag{5}$$

Hence, the maximum possible peak spectral acceleration value is always equal to 2PFA, independently on the floor considered. It is worth noting that, in this case, the maximum peak spectral acceleration value depends on the "absolute" value of T_a, that is, it does not depend on T_a/T_1 ratio.

As above shown, the previous code prescriptions generally relate the PFA linear or multilinear distribution along the building height to the floor height normalized with respect to the building height (*i.e.*, the higher Z/H, the higher the PFA) and the FRS shape to the ratio between the T_a and T_1. From both these features, it can be assumed that they relate the FRS to the elastic response of the structure to its first vibration mode.

The Commentary (Circolare 2019) to the current Italian building code proposes three different expressions to compute FRS. The first two expressions are addressed to the seismic assessment of nonstructural elements or local mechanisms, while the third one refers specifically to framed RC structures. The first expression is based on a "rigorous" approach, while the second and third

expressions are simplified approaches that are borrowed from the work of Degli Abbati et al. 2018 and Petrone et al. 2015, respectively.
All three expressions account for multimodal contributions and the effect on FRS of structural nonlinearity.

The “rigorous” method (defined as Circolare 2019-1) accounts for multimodal contributions based on simple considerations related to structural dynamics. In fact, Eq. (6) gives the contribution of the k^{th} vibration mode to the acceleration FRS at the Z^{th} floor of the building as:

$$S_{aZ,k}(T_a, \xi_a) = PFA_{Z,k} \cdot R\left(\frac{T_a}{T_k}; \xi_a\right) \tag{6}$$

where $PFA_{Z,k}$ is the contribution to the *PFA* given by the k^{th} mode at the Z^{th} building floor, while R is an amplification (or de-amplification) factor of the *PFA* which depends on the natural periods of the main structure (T_k) and on the period and damping feature of the nonstructural element (T_a and ξ_a, respectively).
$PFA_{Z,k}$ is calculated as in Eq. (7):

$$PFA_{Z,k} = \Gamma_k \Phi_{Z,k} S_a(T_k) \tag{7}$$

where Γ_k is the modal participation factor for the k^{th} vibration mode, Φ_k is the modal displacement of the Z^{th} storey for k^{th} vibration mode, $S_a(T_k)$ is the spectral acceleration of the structure associated with its k^{th} vibration period, potentially reduced by means of the structure behavior factor, i.e., q factor in EN1998-1:2004.
R is instead calculated as in Eq. (8):

$$R = \left[\left(2\xi_a \frac{T_a}{T_k}\right)^2 + \left(1 - \frac{T_a}{T_k}\right)^2\right]^{-\beta} \tag{8}$$

where β is a coefficient (ranging from 0.4 and 0.5) which considers the coupling between each building structural mode and the vibration mode of the secondary element. If T_a=T_k, R=1/(2ξ_a) according to Eq. (8) and the maximum value of $S_{aZ,k}$ becomes 1/(2ξ_a) times $PFA_{Z,k}$ in Eq. (6). The result of the maximum amplification is a classical result of the dynamic of the damped SDOF system, even if obtained with a slightly different and less rigorous formulation. For each storey, the floor spectrum is finally obtained as a combination of multimodal contributions through the Square Root of Sum of the Squares (SRSS) rule. Thus, it has a spectral shape with multiple peaks corresponding to the number of significant modes considered.
It may appear quite surprising that a theoretical formulation referring to a harmonic motion appears in a code. Also, due to its nature, Eq. (6) is expected to provide significantly overestimated values of the real maximum PSA.

The Commentary (Circolare 2019) to the current Italian building code proposes also a "simplified" analytical formulation for nonstructural elements and local mechanisms. This formulation (defined as Circolare 2019-2) allows computing the acceleration floor spectrum $S_{aZ}(T,\xi)$ at the level Z where the element is placed as the SRSS combination rule of the contribution provided by all the relevant modes considered (Eq. (9)). The expression is based on the dynamic properties of the main structure (natural periods T_k, modal participation factor Γ_k and modal displacement Φ_k for the k^{th} vibration mode) and on the value of the seismic response spectrum at the base of the building in correspondence of the natural periods $S_a(T_k)$. Moreover, it depends on the damping features of the main structure (ξ_k, related to the k^{th} mode) and on the features of the NSC, introduced through the damping correction factor $\eta(\xi_a)$ computed by Eq. (12).

$$S_{aZ}(T_a,\xi_a,Z) = \sqrt{\sum (S_{aZ,k}(T_a,\xi_a))^2} \ (\geq S_a(T_a,\xi_a) \ for\ T_a > T_1) \tag{9}$$

Eq. (10) and Eq. (11) give the contribution provided by the k^{th} mode of the main structure, respectively to the floor spectrum and the *PFA*.

$$S_{aZ,k}(T_a,\xi_a,Z) = \begin{cases} \dfrac{1.1\xi_k^{-0.5}\eta(\xi_a)PFA_{Z,k}(Z)}{1+\left[1.1\xi_k^{-0.5}\eta(\xi_a)-1\right]\left(1-\dfrac{T_a}{aT_k}\right)^{1.6}} & for\ T_a < aT_K \\ 1.1\xi_k^{-0.5}\eta(\xi_a)PFA_{Z,k}(Z) & for\ aT_k \leq T_a < bT_k \\ \dfrac{1.1\xi_k^{-0.5}\eta(\xi_a)PFA_{Z,k}(Z)}{1+\left[1.1\xi_k^{-0.5}\eta(\xi_a)-1\right]\left(\dfrac{T_a}{bT_k}-1\right)^{1.2}} & for\ T_a \geq bT_k \end{cases} \tag{10}$$

$$PFA_{Z,k}(Z) = S_a(T_k,\xi_k)|\Gamma_k\Phi_k(Z)|\sqrt{1+4\xi_k^2} \tag{11}$$

$$\eta(\xi_a) = \sqrt{\frac{0.1}{0.05+\xi_a}} \geq 0.55 \tag{12}$$

The two coefficients *a* and *b* in Eq. (10) define the range of maximum amplification of the floor spectrum; they can be assumed respectively equal to 0.8 and 1.1. They are introduced to define a plateau of maximum amplification and overcome in this way the uncertainties related to the identification of the structure's natural periods. Finally, the expression allows considering the decrease of amplification due to nonlinearity using an equivalent viscous damping ξ_k and an elongated equivalent period T_k.

The Commentary (Circolare 2019) to the current Italian building code finally proposes another "simplified" formulation in Eq. (13) (defined as Circolare 2019-3 hereinafter), specifically addressed to framed reinforced concrete structures.

$$S_a(T_a) = \begin{cases} PGA\left(1+\frac{Z}{H}\right)\left[\frac{a_p}{1+(a_p-1)\left(1-\frac{T_a}{aT_1}\right)^2}\right] \geq PGA \quad for\ T_a < aT_1 \\ PGA\left(1+\frac{Z}{H}\right)a_p \qquad\qquad for\ aT_1 \leq T_a < bT_1 \\ PGA\left(1+\frac{Z}{H}\right)\left[\frac{a_p}{1+(a_p-1)\left(1-\frac{T_a}{bT_1}\right)^2}\right] \geq PGA \quad for\ T_a \geq bT_1 \end{cases} \tag{13}$$

In Eq. (13), a, b, and a_p are coefficients depending on T_1 that account for higher modes effects (the coefficient a), resonance period elongation due to nonlinearity (the coefficient b) and effect of nonlinearity on the maximum value of the spectral acceleration (the coefficient a_p). If T_a equals zero, a linear PFA distribution along the building height is obtained. PFA ranges from PGA (at Z equal to zero) to 2PGA (at Z equal to H). On the other hand, the maximum value of $S_a(T_a)$ is obtained if T_a is between aT_1 and bT_1. In this case, the FRS acceleration ranges from 2.5PFA to 5PFA, dependently on a_p value.

Table 5 summarizes the expressions proposed in the examined codes. Generally, FRS obtained by applying the code prescriptions above illustrated are determined by two parts: (i) a distribution of the PFA along the building height and (ii) a spectral shape function amplifying or deamplifying the PFA to obtain the peak spectral acceleration. This spectral shape can be fixed or different, in terms of maximum amplification and resonance period, from floor to floor. There are different significant parameters influencing both the PFA and the spectral shape function, above all the effect of higher vibration mode and structural nonlinearity. Not all the above listed proposals account for all these parameters, as summarized in Table 6.

It is worth noting that none of the proposals explicitly refers to infilled buildings as if the presence of infills could only be considered through T_1 value, namely as if the presence of infills only affects the resonance period at which the maximum PSA is attained, except for the simplified proposal of the Italian regulation (Circolare 2019-3). In the last proposal, the maximum PSA value also depends on T_1 and attains it maximum potential value for small values of the period (i.e., a_p = 5 when T_1 is lower than 0.5 seconds). In other words, based on this approach, an infilled building is expected to experience a maximum PSA value at a certain floor equal or higher than the value predicted for an identical building without infills.

Table 5. Summary of code proposals.

Code	Equation	Id
EC8	$S_{a,Z}(T_a) = \mathrm{PGA}\left[\frac{3(1+\mathrm{Z/H})}{1+(1-\mathrm{T_a/T_1})^2} - 0.5\right] \geq \mathrm{PGA}$	(1)
ASCE/SEI 7-10	$S_{a,Z} = \mathrm{PGA}\left(1 + 2\frac{\mathrm{Z}}{\mathrm{H}}\right)\mathrm{a_p}$	(2)
NZSEE2017	$S_{a,Z}(T_a) = \mathrm{PGAC_{Hi}C_i(T_a)}$	(3)
	$\mathrm{C}_{Hi} = \begin{cases} 1+\frac{\mathrm{Z}}{6} & for\ all\ Z < 12m \\ 1+10\frac{\mathrm{Z}}{H} & for\ Z < 0.2H \\ 3.0 & for\ Z \geq 0.2H \end{cases}$	(4)
	$C_i(T_a) = \begin{cases} 2, & for\ T_a \leq 0.5\ s \\ 2\left(\frac{0.5}{T_a}\right)^{0.75}, & for\ 0.5\ s < T_a < 1.5\ s \\ 1.32/T_a, & for\ 1.5\ s < T_a < 3\ s \\ 3.96/{T_a}^2, & for\ T_a \geq 3\ s \end{cases}$	(5)
Circolare 2019-1 "rigorous"	$S_{aZ,k}(T_a,\xi_a) = PFA_{Z,k}\cdot R\left(\frac{T_a}{T_k};\xi_a\right)$	(6)
	$PFA_{Z,k} = \Gamma_k\Phi_{Z,k}S_a(T_k)$	(7)
	$R = \left[\left(2\xi_a\frac{T_a}{T_k}\right)^2 + \left(1-\frac{T_a}{T_k}\right)^2\right]^{-\beta}$	(8)
Circolare 2019-2 "simplified"/ Degli Abbati et al.	$S_{aZ}(T_a,\xi_a,Z) = \sqrt{\sum(S_{aZ,k}(T_a,\xi_a))^2}\ \ (\geq S_a(T_a,\xi_a)\ \ for\ T_a > T_1)$	(9)
	$S_{aZ,k}(T_a,\xi_a,Z) = \begin{cases} \frac{1.1\xi_k^{-0.5}\eta(\xi_a)PFA_{Z,k}(Z)}{1+\left[1.1\xi_k^{-0.5}\eta(\xi_a)-1\right]\left(1-\frac{T_a}{aT_k}\right)^{1.6}} & for\ T_a < aT_K \\ 1.1\xi_k^{-0.5}\eta(\xi_a)PFA_{Z,k}(Z) & for\ aT_k \leq T_a < bT_k \\ \frac{1.1\xi_k^{-0.5}\eta(\xi_a)PFA_{Z,k}(Z)}{1+\left[1.1\xi_k^{-0.5}\eta(\xi_a)-1\right]\left(\frac{T_a}{bT_k}-1\right)^{1.2}} & for\ T_a \geq bT_k \end{cases}$	(10)
	$PFA_{Z,k}(Z) = S_a(T_k,\xi_k)\lvert\Gamma_k\Phi_k(Z)\rvert\sqrt{1+4\xi_k^2}$	(11)
	$\eta(\xi_a) = \sqrt{\frac{0.1}{0.05+\xi_a}} \geq 0.55$	(12)
Circolare 2019-3 "simplified"/ Petrone et al.	$S_a(T_a) = \begin{cases} PGA\left(1+\frac{Z}{H}\right)\left[\frac{a_p}{1+(a_p-1)\left(1-\frac{T_a}{aT_1}\right)^2}\right] \geq PGA & for\ T_a < aT_1 \\ PGA\left(1+\frac{Z}{H}\right)a_p & for\ aT_1 \leq T_a < bT_1 \\ PGA\left(1+\frac{Z}{H}\right)\left[\frac{a_p}{1+(a_p-1)\left(1-\frac{T_a}{bT_1}\right)^2}\right] \geq PGA & for\ T_a \geq bT_1 \end{cases}$	(13)

Table 6. Influencing parameters considered in the code proposals.

	EC8	ASCE/SEI 7-10	NZSEE2017	Circolare 2019-1	Circolare 2019-2	Circolare 2019-3
PFA profile shape	Linear	Linear	Multilinear	Combination of mode shapes	Combination of mode shapes	Linear
Floor-dependent spectral shape	✓	No	No	✓	✓	No
Higher modes	No	No	No	✓	✓	✓ (1)
Structural nonlinearity	No	No	No	✓ (2)	✓	✓ (1)
NSC nonlinearity	No	No	No	✓	✓	No

(1) The parameters a,b, and a_p are calibrated to consider structural nonlinearity and higher mode contribution.

(2) The structural nonlinearity can be considered through a behavior factor.

4 References

Adam C, Fotiu PA. (2000). Dynamic analysis of inelastic primary-secondary systems. Engineering Structures, 22(1):58-71. URL: https://doi.org/10.1016/S0141-0296(98)00073-X

Adam C, Furtmüller T. (2008a). Seismic response characteristics of nonstructural elements attached to inelastic buildings. Proceeding of 7th European Conference on Structural Dynamics (EURODYN 2008), July 7-9, Southampton, UK. Paper N. 120.

Adam C, Furtmüller T. (2008b). Response of nonstructural components in ductile load-bearing structures subjected to ordinary ground motions. Proceeding of 14th World Conference on Earthquake Engineering (14WCEE), October 12-17, Beijing, China.

Adam C, Furtmüller T, Moschen L. (2013). Floor Response Spectra for Moderately Heavy Nonstructural Elements Attached to Ductile Frame Structures. In: Papadrakakis, M., Fragiadakis, M., Plevris, V. (eds) Computational Methods in Earthquake Engineering. Computational Methods in Applied Sciences, 30:69-89. Springer, Dordrecht. https://doi.org/10.1007/978-94-007-6573-3_4

Alonso-Rodríguez A, Miranda E. (2015). Assessment of building behavior under near-fault pulse-like ground motions through simplified models. Soil Dynamics and Earthquake Engineering, 79(A):47-58. URL: https://doi.org/10.1016/j.soildyn.2015.08.009

Anagnostopoulos S, Kyrkos M, Stathopoulos K. (2015). Earthquake induced torsion in buildings: critical review and state of the art. Earthquakes and Structures 8(2):305–377. URL: https://doi.org/10.12989/eas.2015.8.2.305

Anajafi H. (2018). Improved seismic design of non-structural components (NSCs) and development of innovative control approaches to enhance the seismic performance of buildings and NSCs. Ph.D. Dissertation. University of New Hampshire, NH, USA. URL: https://pqdtopen.proquest.com/pubnum/10935426.html

Anajafi H, Medina RA. (2019). Lessons Learned from Evaluating the Responses of Instrumented Buildings in the United States: The Effects of Supporting Building Characteristics on Floor Response Spectra. Earthquake Spectra, 35(1):159–191. URL: https://doi.org/10.1193/081017EQS159M

Anajafi H, Medina RA, Santini-Bell E. (2020). Inelastic floor spectra for designing anchored acceleration-sensitive nonstructural components. Bulletin of Earthquake Engineering, 18(5):2115-2147. URL: https://doi.org/10.1007/s10518-019-00760-8

Anajafi H, Medina RA, Adam C. (2022). Evaluation of the Floor Acceleration Response Spectra of Numerical Building Models Based on Recorded Building Response Data, Journal of Earthquake Engineering 26:12, 6378-6402. URL: https://doi.org/10.1080/13632469.2021.1927887

ASCE/SEI7-10. Minimum Design Loads for Buildings and Other Structures. ASCE7 10. Reston,VA: ASCE;2010.

Asfura A, Der Kiureghian A. (1986). Floor response spectrum method for seismic analysis of multiply supported secondary systems. Earthquake Engineering and Structural Dynamics, 14(2):245-265. URL: https://doi.org/10.1002/eqe.4290140206

Asgarian A, McClure G. (2014). Impact of seismic rehabilitation and presence of unreinforced Masonry (URM) infill walls on the dynamic characteristics of a hospital building in Montreal. Canadian Journal of Civil Engineering, 41(8):748-760. URL: https://doi.org/10.1139/cjce-2013-0092

Bernal D, Cabrera E, Rodríguez E. (2014). Diaphragm Flexibility in Floor Spectra, In: Foss, G., Niezrecki, C. (eds) Special Topics in Structural Dynamics, Volume 6. Conference Proceedings of the Society for Experimental Mechanics Series. Springer, Cham, New York, 355–359. URL: https://doi.org/10.1007/978-3-319-04729-4_31

Blasi G, Perrone D, Aiello MA. (2018). Fragility functions and floor spectra of RC masonry infilled frames: influence of mechanical properties of masonry infills. Bulletin of Earthquake Engineering, 16(12):6105-6130. URL: https://doi.org/10.1007/s10518-018-0435-4

Çelebi M, Bongiovanni G, Şafak E, Brady AG. (1989). Seismic response of a large-span roof diaphragm, Earthquake Spectra 5(2):337–350. URL: https://doi.org/10.1193/1.1585525

CESMD [Center for Engineering Strong-Motion Data]. 2019. Accessed May 8, 2019. https://trongmotioncenter.org/.

Circolare 2019. Circolare esplicativa delle Norme Tecniche per le Costruzioni. Supplemento ordinario n.5 Gazzetta Ufficiale 11 febbraio, 2019 (in Italian).

Chaudhuri SR, Villaverde R. (2008). Effect of building nonlinearity on seismic response of nonstructural components: a parametric study. Journal of Structural Engineering 134(4):661–670. URL: https://doi.org/10.1061/(ASCE)0733-9445(2008)134:4(661)

Chaudhari SR, Hutchinson TC. (2011). Effect of building nonlinearity of frame buildings on peak horizontal floor acceleration. Journal of Earthquake Engineering 15(1):124-142. URL: https://doi.org/10.1080/13632461003668046

Chen Y, Soong TT. (1988). State-of-the-art review seismic response of secondary systems. Engineering Structures, 10(4):218-228. URL: https://doi.org/10.1016/0141-0296(88)90043-0

Cohen GL, Kilngner RE, Hayes, JR Jr, Sweeney SC. (2001). Seismic Response of Low- Rise Masonry Buildings with Flexible Roof Diaphragms, Corps of Engineers, Washington, DC.

Degli Abbati S, Cattari S, Lagomarsino S. (2018). Theoretically-based and practice-oriented formulations for the floor response spectra evaluation. Earthquake Structures. 15(5):565-581. URL: https://doi.org/10.12989/eas.2018.15.5.565

Derakhshan H, Nakamura Y, Griffith MC, Ingham JM. (2022). Suitability of Height Amplification Factors for Seismic Assessment of Existing Unreinforced Masonry Components, Journal of Earthquake Engineering 26(3):1347-1366. URL: https://doi.org/10.1080/13632469.2020.1716889

Di Domenico M, Ricci P, Verderame GM. (2021). Floor spectra for bare and infilled reinforced concrete frames designed according to Eurocodes. Earthquake Engineering and Structural Dynamics 50(13):3577–3601. URL: https://doi.org/10.1002/eqe.3523

Eurocode 8. (2004). Design of Structures for Earthquake Resistance. Part 1-1: General Rules, Seismic Actions and Rules for Buildings. Brussels.

FEMA 356. (2000). Pre-standard and commentary for the seismic rehabilitation of building.

FEMA P-695. (2009). Quantification of building seismic performance factors. Prepared by the Applied Technology Council for the Federal Emergency Management Agency, Washington, D.C., USA.

Filiatrault A, Sullivan TJ. (2014). Performance-based seismic design of nonstructural building components: the next frontier of earthquake engineering. Earthquake Engineering and Engineering Vibrations 13(Suppl 1):17-46. URL: https://doi.org/10.1007/s11803-014-0238-9

Fleischman RB, Sause R, Pessiki S, Rhodes AB. (1998). Seismic behavior of precast parking structure diaphragms, PCI Journal 43(1):38–53. URL: https://doi.org/10.15554/pcij.01011998.38.53

Fleischman RB, Farrow KT. (2001). Dynamic behavior of perimeter lateral-system structures with flexible diaphragms. Earthquake Engineering and Structural Dynamics 30(5):745–763. URL: https://doi.org/10.1002/eqe.36

Fleischman RB, Farrow KT, Eastman K. (2002). Seismic performance of perimeter lateral-system structures with highly flexible diaphragms. Earthquake Spectra 18(2):251–286. URL: https://doi.org/10.1193/1.1490547

Floros A. (2006). Distribution of earthquake-induced floor horizontal accelerations and generation of floor response spectra for inelastic R.C. frames. M.Sc. Thesis, ROSE School, Pavia, Italy.

Francis TC, Hendry BC, Sullivan TJ. (2017). Vertical spectral demands on building elements induced by earthquake excitation. Proceedings of the 2017 New Zealand Society for Earthquake Engineering (NZSEE) Annual Conference, April 27-29, Wellington, New Zealand.

Gremer N, Adam C, Medina RA, Moschen L. (2019). Vertical peak floor accelerations of elastic moment-resisting steel frames. Bulletin of Earthquake Engineering, 17(6):3233-3254. URL: https://doi.org/10.1007/s10518-019-00576-6

Gremer N, Moschen L, Adam C, Medina RA. (2018). Horizontal and vertical acceleration demand on moment-resisting steel frames. Proceedings of the 16th European Conference on Earthquake Engineering (16ECEE), June 18-21, Thessaloniki, Greece.

Gupta VK. (1997). Acceleration transfer function of secondary systems. ASCE Journal of Engineering Mechanics, 123(7):678-685. URL: https://doi.org/10.1061/(ASCE)0733-9399(1997)123:7(678)

Guzman Pujols JC, Ryan KL. (2020). Slab vibration and horizontal-vertical coupling in the seismic response of low-rise irregular base-isolated and conventional buildings. Journal of Earthquake Engineering, 24(1):1-36. URL: https://doi.org/10.1080/13632469.2017.1387197

Ibarra LF, Medina RA, Krawinkler H. (2005). Hysteretic models that incorporate strength and stiffness deterioration. Earthquake Engineering and Structural Dynamics, 34(12):1489-1511. URL: https://doi.org/10.1002/eqe.495

Igusa T, Der Kiureghian A. (1985a). Dynamic characterization of two-degree-of-freedom equipment-structure systems. ASCE Journal of Engineering Mechanics, 111(1):1-19. URL: https://doi.org/10.1061/(ASCE)0733-9399(1985)111:1(1)

Igusa T, Der Kiureghian A. (1985b). Dynamic response of multiply supported secondary systems. ASCE Journal of Engineering Mechanics, 111(1):20-41. URL: https://doi.org/10.1061/(ASCE)0733-9399(1985)111:1(20)

Igusa T, Der Kiureghian A. (1985c). Generation of floor response spectra including oscillator-structure interaction. Earthquake Engineering and Structural Dynamics, 13(5):661-676. URL: https://doi.org/10.1002/eqe.4290130508

Iverson JK, Hawkins NM. (1994). Performance of precast/prestressed building structures during Northridge earthquake, PCI Journal 39(2):38-56. URL: https://search.worldcat.org/it/title/12789822

Jain A, Surana M. (2022). Floor displacement-based torsional amplification factors for seismic design of acceleration-sensitive non-structural components in torsionally irregular RC buildings. Engineering Structures 254:113871. URL: 10.1016/j.engstruct.2022.113871.

Kanee ART, Kani IMZ, Noorzad A. (2013). Elastic floor response spectra of nonlinear frame structures subjected to forward-directivity pulses of near-fault records. Earthquakes and Structures, 5(1):49-65. URL: https://doi.org/10.12989/eas.2013.5.1.049

Kazantzi AK, Miranda E, Vamvatsikos D. 2020a. Strength-reduction factors for the design of light nonstructural elements in buildings. Earthquake Engineering and Structural Dynamics, 49(13):1329-1343. URL: https://doi.org/10.1002/eqe.3292

Kazantzi AK., Vamvatsikos D, Miranda E. (2020b). Evaluation of seismic acceleration demands on building nonstructural elements. ASCE Journal of Structural Engineering, 146(7). URL: https://doi.org/10.1061/(ASCE)ST.1943-541X.0002676

Kollerathu JA, Menon A. (2017). Role of diaphragm flexibility modelling in seismic ana- lysis of existing masonry structures. Structures 11:22–39. URL: https://doi.org/10.1016/j.istruc.2017.04.001

Kunnath SK, Panahshahi N, Reinhorn AM. (1991). Seismic response of RC buildings with inelastic floor diaphragms. Journal of Structural Engineering 117(4):1218–1237. URL: https://doi.org/10.1061/(ASCE)0733-9445(1991)117:4(1218)

Landge MV, Ingle RK. (2021). Comparative study of floor response spectra for regular and irregular buildings subjected to earthquake. Asian Journal of Civil Engineering 22:49–58.

Landge MV, Ingle RK. (2022). Influence of torsional irregularity on tri-directional floor response spectra used in industrial buildings. Innovative Infrastructure Solutions 7:34. URL: https://doi.org/10.1007/s41062-021-00639-1

Lignos DG, Krawinkler H. (2010). A steel database for component deterioration of tubular hollow square steel columns under varying axial load for collapse assessment of steel structures under earthquakes. Proceedings of the 7th International Conference on Urban Earthquake Engineering (7CUEE) and 5th International Conference on Earthquake Engineering (5ICEE), March 3-5, Tokyo, Japan.

Lim E, Chouw N. (2014). Consequence of main-secondary structures interaction for seismic response of secondary structures. Proceedings of the Annual New Zealand Society of Earthquake Engineering Conference, March 21-23, Auckland, New Zealand.

Lim E, Chouw N. (2018). Prediction of the response of secondary structures under dynamic loading considering primary-secondary structure interaction. Advances in Structural Engineering, 21(14):2143-2153. URL: https://doi.org/10.1177/1369433218768563

Lin J, Mahin SA. (1985). Seismic response of light subsystems on inelastic structures. Journal of Structural Engineering 111(2):400–417. URL: https://doi.org/10.1061/(ASCE)0733-9445(1985)111:2(400

Lucchini A, Mollaioli F, Bazzurro P. (2014). Floor response spectra for bare and infilled reinforced concrete frames. Journal of Earthquake Engineering, 18(7):1060-1082. URL: https://doi.org/10.1080/13632469.2014.916633

Magliulo G, D'Angela D. (2024). Seismic response and capacity of inelastic acceleration-sensitive nonstructural elements subjected to building floor motions. Earthquake Engineering and Structural Dynamics, 53(4):1421-1445. URL: https://doi.org/10.1002/eqe.4080

Mavroeidis GP, Papageorgiou AS. (2003). A mathematical representation of near-fault ground motions. Bulletin of the Seismological Society of America, 93(3):1099-1131. URL: https://doi.org/10.1785/0120020100

Mavroeidis GP, Dong G, Papageorgiou AS. (2004). Near-fault ground motions, and the response of elastic and inelastic single-degree-of-freedom (SDOF) systems. Earthquake Engineering and Structural Dynamics, 33(9):1023-1049. URL: https://doi.org/10.1002/eqe.391

Menon A, Magenes G. (2011a). Definition of seismic input for out-of-plane response of masonry walls: I. parametric study. Journal of Earthquake Engineering 15(2):165-194. URL: https://doi.org/10.1080/13632460903456981

Menon A, Magenes G. (2011b). Definition of seismic input for out-of-plane response of masonry walls: II. Formulation, Journal of Earthquake Engineering 15(2):195-213. URL: https://doi.org/10.1080/13632460903494446

Miranda E, Kazantzi Ak, Vamvatsikos D. (2018). New approach to the design of acceleration-sensitive non-structural elements in buildings. Proceedings on the 16th European Conference on Earthquake Engineering (16ECEE), June 18-21, Thessaloniki, Greece.

Miranda E, Taghavi S. (2005). Approximate floor acceleration demands in multistory buildings. I: formulation. ASCE Journal of Structural Engineering, 131(2):203-211. URL: https://doi.org/10.1061/(ASCE)0733-9445(2005)131:2(203)

Mollaioli F, Lucchini A, Bruno S, De Sortis A, Bazzurro P. (2010). Floor acceleration demand in reinforced concrete frame structures with masonry infill walls. Proceedings on the 9th US National and 10th Canadian Conference on Earthquake Engineering, July 25-29, Toronto, Canada.

Moschen L, Medina RA, Adam C. (2015). Vertical acceleration demands on nonstructural components in buildings. Proceedings of the 5th ECCOMAS Thematic Conference on Computational Methods in Structural Dynamics and Earthquake Engineering (COMPDYN 2015), May 25–27, Crete Island, Greece. Paper C497. URL: https://doi.org/10.7712/120115.3473.497

Moschen L, Medina RA, Adam C. (2016). Vertical acceleration demands on column lines of steel moment-resisting frames. Earthquake Engineering and Structural Dynamics, 45(12):2039-2060. URL: https://doi.org/10.1002/eqe.2751

NTC. Decreto ministeriale 17 gennaio 2018 —Norme Tecniche per le Costruzioni. *Supplemento ordinario n.42 Gazzetta Ufficiale 20 febbraio*, 2018 (in Italian).

NZSEE. New Zealand Society for Earthquake Engineering (NZSEE), Structural Engineering Society New Zealand Inc. (SESOC), New Zealand Geotechnical Society Inc., Ministry of Business, Innovation and Employment, Earthquake Commission. The Seismic Assessment of Existing Buildings (the Guidelines), Part C—Detailed Seismic Assessment; 2017. http://www.eq-assess.org.nz/.

NZS. Structural design actions. Earthquake Design Actions. New Zealand Society for Earthquake Engineering (NZSEE),1170.5:2004.

Obando JC, Lopez-Garcia D. (2018). Inelastic displacement ratios for nonstructural components subjected to floor accelerations. Journal of Earthquake Engineering, 22(4):569-594. URL: https://doi.org/10.1080/13632469.2016.1244131

Pan X, Zheng Z, Wang Z. (2017). Amplification factors for design of nonstructural components considering the near-fault pulse-like ground motions. Bulletin of Earthquake Engineering, 15(4):1519-1541. URL: https://doi.org/10.1007/s10518-016-0031-4

Perrone D, Calvi PM, Nascimbene R, Fischer EC, Magliulo G. (2019). Seismic performance of non-structural elements during the 2016 Central Italy earthquake. Bulletin of Earthquake Engineering 17:5655-5677. URL: https://doi.org/10.1007/s10518-018-0361-5

Petrone C, Magliulo G, Manfredi G. (2015). Seismic demand on light acceleration-sensitive nonstructural components in European reinforced concrete buildings. Earthquake Engineering and Structural Dynamics. 44(8):1203-1217. URL: https://doi.org/10.1002/eqe.2508

Politopoulos I, Feau C. (2007). Some aspects of floor spectra of 1DOF nonlinear primary structures. Earthquake Engineering and Structural Dynamics 36(8):975–993. URL: https://doi.org/10.1002/eqe.664

Qu B, Goel R, Chadwell C. (2014). Evaluation of ASCE/SEI 7 provisions for determination of seismic demands on nonstructural components. In Proceedings of the Tenth US National Conference on Earthquake Engineering, Anchorage, AK.

Reinhorn AM, Kunnath SK, Panahshahi N. (1988). Modeling of R/C Building Structures with Flexible Floor Diaphragms (IDARC2). National Center for Earthquake Engineering Research, Taipei, Taiwan.

Rodriguez ME, Restrepo JI, Carr AJ. (2002). Earthquake induced floor accelerations in building. Earthquake Engineering and Structural Dynamics 31(3):693–718. URL: https://doi.org/10.1002/eqe.149

Ruggieri S, Vukobratovic V. (2022). Acceleration demands in single-storey RC buildings with flexible diaphragms. Engineering Structures 275(Part A):115276. URL: https://doi.org/10.1016/j.engstruct.2022.115276

Ryan K L, Soroushian S, Maragakis E, Sato E, Sasaki T, Okazaki T. (2016). Seismic simulation of an integrated ceiling-partition wall-piping system at E-defense. I: Three-dimensional structural response and base isolation. Journal of Structural Engineering 142(2):04015130. URL: https://doi.org/10.1061/(ASCE)ST.1943-541X.0001385

Sackman JL, Kelly JM. (1979). Seismic analysis of internal equipment and components in structures. Engineering Structures, 1(4):179-190. URL: https://doi.org/10.1016/0141-0296(79)90045-2

Sadashiva, VK, MacRae GA, Deam BL, Spooner MS. (2012). Quantifying the seismic response of structures with flexible diaphragms. Earthquake Engineering and Structural Dynamics 41(10):1365–1389. URL: https://doi.org/10.1002/eqe.1187

Sankaranarayanan R. (2007). Seismic Response of Acceleration-Sensitive Nonstructural Components Mounted on Moment Resisting Frame Structures. PhD Dissertation, University of Maryland, College Park, MD, USA.

Sankaranarayanan R, Medina RA. (2006). Estimation of seismic acceleration demands of nonstructural components exposed to near-fault ground motions. Proceedings of the First European Conference on Earthquake Engineering and Seismology (1st ECEES), September 3-8, Geneva, Switzerland. Paper N. 1248.

Sankaranarayanan R, Medina RA. (2007). Acceleration response modification factors for non-structural components attached to inelastic moment-resisting frame structures. Earthquake Engineering and Structural Dynamics 36(14):2189–2210. URL: https://doi.org/10.1002/eqe.724

Sankaranarayanan R, Medina RA. (2008). Statistical models for a proposed acceleration-response modification factor for nonstructural components attached to inelastic structures. In Proceedings of 14th World Conference on Earthquake Engineering (WCEE), Beijing, China.

Sewell RT, Cornell CA, Toro GR, McGuire RK. (1986). A study of factors influencing floor response spectra in non-linear MDOF structures. *Report No.: 82*, John A. Blume Earthquake Engineering Centre, Civil and Environmental Engineering Dept., Stanford University, Stanford, California. URL: http://purl.stanford.edu/vf765pj9489

Somerville PG, Smith NF, Graves RW, Abrahamson NA. (1997). Modification of empirical strong ground motion attenuation relations to include the amplitude and duration effects of rupture directivity. Seismological Research Letters, 68(1):199-222. URL: https://doi.org/10.1785/gssrl.68.1.199

Soroushian S, Maragakis E, Ryan KL, Sato E, Sasaki T, Okazaki T, Mosqueda G. (2016). Seismic simulation of an integrated ceiling-partition wall-piping system at E-Defense. II: evaluation of

nonstructural damage and fragilities. ASCE Journal of Structural Engineering, 142(2). URL: https://doi.org/10.1061/(ASCE)ST.1943-541X.0001385

Suarez LE., Singh MP. (1987). Floor response spectra with structure-equipment interaction effects by a mode synthesis approach. Earthquake Engineering and Structural Dynamics, 15(2):141-158. URL: https://doi.org/10.1002/eqe.4290150202

Sullivan TJ, Calvi PM, Nascimbene R. (2013b). Towards Improved Floor Spectra Estimates for Seismic Design. Earthquakes and Structures 4(1):109–132. URL: https://doi.org/10.12989/eas.2013.4.1.109

Surana M, Singh Y, Lang DH. (2018a). Floor spectra of inelastic rc frame buildings considering ground motion characteristics. Journal of Earthquake Engineering, 22(3):488-519. URL: https://doi.org/10.1080/13632469.2016.1244134

Surana M, Pisode M, Singh Y, Lang DH. (2018b). Effect of URM infills on inelastic floor response of RC frame buildings. Engineering Structures, 175(15):861-878. URL: https://doi.org/10.1016/j.engstruct.2018.08.078

Swanson EJ, Chen Z, Sprague HO. (2012). Seismic spectra and response analysis for raised access floor and computer equipment systems considering vertical ground motions. ASCE Structures Congress, March 29-31, Chicago, Illinois, USA. pp. 1361-1372. URL: https://doi.org/10.1061/9780784412367.122

Taghavi S, Miranda E. (2008). Effect of interaction between primary and secondary systems on floor response spectra. Proceedings of the 14th World Conference on Earthquake Engineering (14WCEE), October 12-17, Beijing, China.

Tamura I, Matsuura S, Shimazu R. (2016). Yield strength reduction factor of nonlinear SDOF systems on the supporting structures. Proceedings of the ASME 2016 Pressure Vessels and Piping Conference (PVP2016), July 17-21, Vancouver, British Columbia, Canada.

Tena-Colunga A, Abrams DP. (1996). Seismic behavior of structures with flexible diaphragms. Journal of Structural Engineering 122(4):439–445. URL: https://doi.org/10.1061/(ASCE)0733-9445(1996)122:4(439)

Tena-Colunga A, Chinchilla-Portillo KL, Juárez-Luna G. (2015). Assessment of the diaphragm condition for floor systems used in urban buildings. Engineering Structures 93:70–84. URL: https://doi.org/10.1016/j.engstruct.2015.03.025

Toro GR, McGuire RK, Cornell CA, Sewell RT. (1989). Linear and nonlinear response of structures and equipment to California and Eastern United States earthquakes. Electric Power Research Inst, Palo Alto.

Vela RJM, Brunesi E, Nascimbene R. (2018). Derivation of floor acceleration spectra for an industrial liquid tank supporting structure with braced frame systems. Engineering Structures, 171(15):105-122. URL: https://doi.org/10.1016/j.engstruct.2018.05.053

Vela RJM, Brunesi E, Nascimbene R. (2019). Floor spectra estimates for an industrial special concentrically braced frame structure. Journal of Pressure Vessel Technology, 141(1): 010909. URL: https://doi.org/10.1115/1.4041285

Vukobratovic V, Fajfar P. (2017). Code-oriented floor acceleration spectra for building structures. Bulletin of Earthquake Engineering, 15(7):3013-3026. URL: https://doi.org/10.1007/s10518-016-0076-4

Vukobratovic V, Fajfar P. (2024). Direct floor response spectra for nonlinear nonstructural components. Bulletin of Earthquake Engineering, 22(3):1033-1053. URL: https://doi.org/10.1007/s10518-023-01818-4

Wang T, Shang Q, Li J. (2021). Seismic force demands on acceleration-sensitive nonstructural components: a state-of-the-art review. Earthquake Engineering and Engineering Vibrations 20:39-62. URL: https://doi.org/10.1007/s11803-021-2004-0

Zhai CH, Zheng Z, Li S, Pan XL, Xie LL. (2016). Seismic response of nonstructural components considering the near-fault pulse-like ground motions. Earthquakes and Structures, 10(5):1213-1232. URL: https://doi.org/10.12989/eas.2016.10.5.1213

5 List of references included in the experimental database (listed in reverse chronological order)

Xiao J, Kwon OS, Bentz E, Jung JW, Kim M. (2024). Effect of modeling assumptions on predicting seismic responses of a three-story reinforced concrete shear wall structure. Earthquake Engineering and Structural Dynamics 53(1):414-431. URL: https://doi.org/10.1002/eqe.4026

Wu H, Guo E, Wang J, Dai X, Dai C. (2024). Seismic performance evaluation of water supply pipes installed in a full-scale RC frame structure based on a shaking table test. Earthquake Engineering and Engineering Vibrations 23:163-178. URL: https://doi.org/10.1007/s11803-024-2232-1

Wu H, Guo E, Sun D, Mao C, Zhang H, Liu Z. (2022). Shaking Table Test of Water Supply Pipes Installed in a Full-Scale Masonry Structure. KSCE Journal of Civil Engineering 26:824–836. URL: https://doi.org/10.1007/s12205-021-5586-1

Zou X,·Yang W,·Liu P, Wang M. (2023) Floor acceleration amplification and response spectra of reinforced concrete frame structure based on shaking table tests and numerical study. Archives of Civil and Mechanical Engineering 23:156. URL: https://doi.org/10.1007/s43452-023-00648-0

Lei Y, Shang Q, Song W, Yu Y, Pan P, Wang T. (2023). Shaking table tests of base-isolated reinforced concrete frame by double friction pendulum bearings. Journal of Building Engineering 69:106240. URL: https://doi.org/10.1016/j.jobe.2023.106240

Butenweg C, Bursi OS, Paolacci F, Marinković M, Lanese I, Nardin C., Quinci G. (2021). Seismic performance of an industrial multi-storey frame structure with process equipment subjected to shake table testing. Engineering Structures 243:112681. URL: https://doi.org/10.1016/j.engstruct.2021.112681

Vukobratović V, Yeow TZ, Kusunoki K. (2021). Floor acceleration demands in three RC buildings subjected to multiple excitations during shake table tests. Bulletin of Earthquake Engineering 19:5495-5523. URL: https://doi.org/10.1007/s10518-021-01181-2

Crozet V, Politopoulos I, Chaudat T. (2019). Shake table tests of structures subject to pounding. Earthquake Engineering and Structural Dynamics 48(10):1156-1173. URL: https://doi.org/10.1002/eqe.3180

Chakraborty S, Ray-Chaudhuri S. (2017). Energy transfer to high-frequency modes of a building due to sudden change in stiffness at its base. Journal of Engineering Mechanics 143(8):04017050. URL: https://doi.org/10.1061/(ASCE)EM.1943-7889.0001262

Kothari P, Parulekar YM, Reddy GR, Gopalakrishnan N. (2017). In-structure response spectra considering nonlinearity of RCC structures: Experiments and analysis. Nuclear Engineering and Design 322:379-396. URL: https://doi.org/10.1016/j.nucengdes.2017.07.009

Zhang C, Jiang NA. (2017). Shaking Table Real-Time Substructure Experiment of An Equipment–Structure–Soil Interaction System. Advances in Mechanical Engineering 9(10). URL: https://doi.org/10.1177/1687814017724090

Zhang C, Jiang NA. (2017). Effects of Equipment- Structure-Soil Interaction on Seismic Response of Equipment and Structure via Real-Time Dynamic Substructuring Shaking Table Testing. Shock and Vibration 2017:1291265. URL: https://doi.org/10.1155/2017/1291265

Ryan K L, Soroushian S, Maragakis E, Sato E, Sasaki T, Okazaki T. (2016). Seismic simulation of an integrated ceiling-partition wall-piping system at E-defense. I: Three-dimensional structural response and base isolation. Journal of Structural Engineering 142(2):04015130. URL: https://doi.org/10.1061/(ASCE)ST.1943-541X.0001385

Beyer K, Tondelli M, Petry S, Peloso S. (2015). Dynamic testing of a four-storey building with reinforced concrete and unreinforced masonry walls: prediction, test results and data set. Bulletin of Earthquake Engineering 13:3015-3064. URL: https://doi.org/10.1007/s10518-015-9752-z

Lepage A, Shoemaker JM, Memari AM. (2012). Accelerations of nonstructural components during nonlinear seismic response of multistory structures. Journal of Architectural Engineering 18(4):285-297. URL: https://doi.org/10.1061/(ASCE)AE.1943-5568.0000087

Tashkov L, Manova K, Krstevska L, Garevski M. (2010). Evaluation of efficiency of ALSC floating-sliding base-isolation system based on shake table test and floor response spectra. Bulletin of Earthquake Engineering 8:995-1018. URL: https://doi.org/10.1007/s10518-009-9158-x

Bothara JK, Dhakal RP, Mander JB. (2010). Seismic performance of an unreinforced masonry building: An experimental investigation. Earthquake Engineering and Structural Dynamics 39(1):45-681. URL: https://doi.org/10.1002/eqe.932